64-2

March 18, 1963

ULTRA HIGH POWER TRANSMISSION LINE TECHNIQUES

Final Technical Note

Contract No. AF30(602)-2545

Rome Air Development Center
Research and Technology Division
Air Force Systems Command
United States Air Force

Griffiss Air Force Base
New York

MICROWAVE ASSOCIATES, INC.

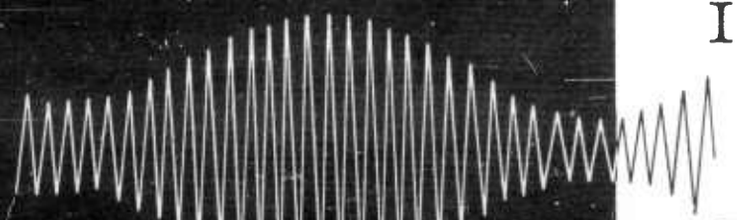

RADC-TDR-63-167 March 18, 1963

ULTRA HIGH POWER TRANSMISSION LINE TECHNIQUES

Prepared by:

Dr. Meyer Gilden

Richard Madore

Joseph Pergola

Approved by:

Dr. Lawrence Gould

MICROWAVE ASSOCIATES, INC.
Burlington, Massachusetts

Final Technical Note

Contract No. AF30(602)-2545

Prepared
for
Rome Air Development Center
Research and Technology Division
Air Force Systems Command
United States Air Force

Griffiss Air Force Base
New York

ABSTRACT

The ultra-high power transmission line techniques including both failure mechanisms and component design are discussed. Failures resulting from localized regions of heated gas were studied and a more general equation for breakdown was derived to show the effect of the size of the region. Similarly small obstacles produce regions of high field strength; but the presence of these very small regions become evident only at high pressures or with high dielectric strength gases. Among the other subjects reviewed from earlier reports is the experimental study of the factors effecting arc movement in a waveguide.

In view of the many advantages of the low loss mode in circular waveguide for ultra-high power levels, a mode transducer and a two section mode filter or suppressor were designed and constructed. The short compact transducer has a bandwidth more than 8 percent and it can handle about 25 percent of the peak power of a standard rectangular waveguide. Water cooling is provided for high average power operation. Analysis of mode suppression as related to failure of waveguide systems indicates that an equivalent one way attenuation of 5 db is a practical value of attenuation for a mode suppressor where high average power levels are involved. Where only high peak powers are involved lower levels of attenuation are sufficient.

Title of Report RADC-TDR-63-167

PUBLICATION REVIEW

This report has been reviewed and is approved.

Approved:

ARTHUR J. FROHLICH
Chief, Techniques Laboratory
Directorate of Aerospace Surveillance & Control

Approved:

WILLIAM T. POPE
Acting Director
Director of Aerospace
Surveillance & Control

FOR THE COMMANDER:

IRVING J. GABELMAN
Director of Advanced Studies

TABLE OF CONTENTS

LIST OF ILLUSTRATIONS

I. INTRODUCTION

Purpose

The purpose of this program is to study ultra-high power transmission line techniques. One aspect of the work covers failure mechanisms at levels of peak power and average power that cannot be transmitted by the standard waveguides in present use. In general, because of the nature of the failure mechanisms, one cannot speak of peak power or average power limitations independently; more specifically, heating effects related to average power can result in significant reduction in the peak power which a system can handle. By obtaining a better understanding of the dependence of the failure mechanisms on the environment in the waveguide and the structure of waveguide components it is hoped that practical solutions of some of the ultra-high power problems will be obtained. Another aspect of the work has been the development of several components for ultra-high power levels. This program is concerned with transmission lines and associated components for frequencies in the range from 1 to 35 kmc.

Scope of the Work

There are four problems which arise in considering ultra-high power levels including electrical breakdown, excessive heating, the nature of the microwave arc (occurring inadvertently in the waveguide), and the electrical characteristics of the necessarily over-sized waveguide structures.

Electrical breakdown in uniform fields or slightly non-uniform

fields has been studied extensively at microwave frequencies[1,2,3]. In this program breakdown theory and experiment are extended to include non-uniform conditions more generally; included are the effects of highly localized increases in electric field near small discontinuities and highly localized reductions in gas density. The latter arises from temperature gradients which are found at excessively hot waveguide windows, at a small foreign body in the waveguide, and at hot localized metallic surfaces. The effect of these non-uniformities in electric field and gas density on electrical breakdown are also dependent upon the gas fill. The important point to note is that it is not sufficient to consider only the maximum value of electric field or just the hottest point in a microwave system. The size of the region also plays a very significant part. Evidence of this factor can be found in the experience with current microwave systems where expected improvements from pressurization including high dielectric strength gases are not realized[4].

The rise of waveguide temperature is also a factor which must be considered for ultra-high power levels. This problem has been analyzed in other concurrent programs[4,5] and so will not be treated in this report; however, some of the decisions are based upon them.

The nature of a microwave arc once it has been inadvertently initiated in the waveguide is an important aspect of the failure problem. While intermittent arcing may not cause serious damage to the transmission line, a heavy continuous arc once formed may not only damage the transmission line but also results in the destruction

of the vacuum window of the ultra-high power tube[6]. The items which govern the nature of the arc including its movement and destructive power are gas fill, the signal characteristics, and the surface conditions of the waveguide itself.

The use of over-sized waveguide and components for ultra-high powers, which has many advantages, brings up a number of problems. The over-riding problem is the suppression of spurious modes so that they do not cause failure, excessive heating, or excessive signal attenuation. An auxiliary matter is the removal of heat that arises from both the attenuation of the main mode of propagation as well as the absorption of the spurious modes of propagation.

These four areas of interest can be treated in general without regard to size or frequency of operation since there is no significant change in the breakdown theory or microwave loss theory over the range of frequencies from 1 to 35 kmc. However, in this range the physical realization of systems may vary considerably depending upon practical considerations. Items which must be considered include, strength of the waveguide, efficient cooling techniques, materials, surface conditions and fabrication techniques.

Contents of Report

In this report, the final report, the previous work is summarized. The subjects include: the derivation of a more general equation for breakdown, an approximate solution for breakdown at a hot surface, experimental breakdown measurements at a small electrical discontinuity, the temperature rise of a foreign body in the waveguide, experimental

observations on moving arcs, the cooling capacity of internal gas flow, and analysis of spurious mode filters. After the summary the report continues with additional theoretical and experimental work on breakdown near a hot surface. The final section of the report treats the design and construction of two components for high power application and presents an analysis demonstrating optimization of spurious mode suppressors or filters.

II. CONCLUSIONS AND RECOMMENDATIONS

The contribution to breakdown of small localized regions of high field strength or elevated gas temperature causes a departure from the simple pressure squared dependence of the breakdown power. For the case of elevated gas temperature near a hot surface, a sufficient flow of cooler gas at the surface increases the breakdown level to that of the cool gas even though a layer of hot gas exists at the surface. This effect is in addition to the possible increase obtained from merely cooling the hot surface. In working with this problem a more general breakdown equation was derived and then solved for conditions applicable to the resonant cavity experiment which was carried out for verification of the theory.

The study of arc movement for high duty cycle or CW conditions showed that the arc movement towards the generator was due mainly to the expansion of the hot ionized portion of the gas. Most important is the fact that a counter-flow of neutral gas could slow down and even reverse the direction of arc motion. An internal gas flow can also cool the components and the waveguide; however, because of the relatively low thermal capacity of gases, the gas temperature would reach equilibrium with the waveguide walls within a few feet in X band waveguide. Thus the air flow down a long waveguide run would have to be broken into short sections. These results and the work on breakdown at a hot surface suggest that a strong counter-flow of gas away from the transmitter should reduce the occurrence of failures and protect components in waveguide systems.

The design and construction of circular waveguide components in the low loss mode leads to a satisfactory solution to many of the failure mechanisms anticipated for super power application. A short mode transducer, $TE_{10}^{\square}$ to TE_{01}° was developed having a bandwidth of 8% and a peak power capability not less than a factor of 4 below what the rectangular waveguide can handle. As part of the design of a short spurious mode suppressor it was concluded that the most important requirement was that the possible resonances of the spurious modes be limited to safe values (i.e., peaks in electric fields must be kept below the breakdown threshold and absorption of power at the spurious modes must be kept low). Also, it was recognized that the mode filter should be evaluated in the presence of a large standing wave in order to include the effect of the relative position of the standing wave pattern to the coupling slots of the mode suppressor. Our analysis shows that a one way absorption of 5 db of the spurious mode by the mode filter is sufficient to limit resonances to a safe level.

III. DISCUSSION

Summary of Previous Work

Ultra-high power transmission line techniques involve detailed consideration of failure mechanisms. Work done in this program and several related programs[4,5] lead to the conclusion that breakdown under highly non-uniform conditions is a key item particularly under inadvertent conditions. See, for example, the breakdown curve, Fig. 1, in Report No. 5 of Reference (4). Good engineering can generally result in components realizing the waveguide power handling capability within a factor of 2 or 3 as opposed to the above problems.

In this program a careful study was made of the electron continuity equation which leads to the breakdown conditions. The result was a more general equation which includes the effect of gradients in gas density, due mainly to gradients in gas temperature in a high power system. The modified condition for CW breakdown was found to be

$$\frac{\nu_n}{D}\Phi\psi + \Phi\nabla^2\psi + \underline{(\nabla\Phi)\ (\nabla\psi)} = 0 \ , \qquad (1)$$

where ν_n is the net ionization coefficient (a function of E/p)

D is the electron diffusion coefficient

$\psi = Dn_e/\Phi$, the normalized electron density

n_e is the electron density

Φ is N_o/N the inverse ratio of the relative gas density. The underlined term is the one which has not appeared before and makes the result more general. Gradients in electric field do not give rise to the extra term and enter primarily through the term ν_n. In both cases, if there are gradients, the differential equation becomes non-linear and ν_n and D are only known emperically. Thus, numerical methods are generally used for solution.

In the preceeding reports a preliminary attack was made on the problem of breakdown near a hot surface using Eq. (1). A more correct solution is given in this report. Other non-uniform breakdown problems included an analysis of the electric field strengths at a rough surface and measurement of breakdown in air at a hemisphere over a wide enough range of pressure to demonstrate the transition from a local breakdown (at high pressures) to a volume breakdown (at low pressures), Fig. 1. The dashed lines show the theoretical uniform field breakdown case.

Several other effects leading to failure were examined in the preceeding reports. Foreign particles inadvertently left inside the waveguide can become extremely hot when high power is present. With the increase in temperature the breakdown threshold in the extreme case is reduced inversely as the square of the absolute temperature ratio. The temperature rise in a practical case is shown in Fig. 2. Arc movement, after a failure, is an important factor in defining the requirements for system protection. The result of our studies of arc movement under high duty cycle conditions with various gases is shown

in Fig. 3. Note that under comparable conditions the arc moves much more slowly for high dielectric strength gases. A most significant result is shown in Fig. 4 where a counter flow of gas was produced. The measurements suggest that the arc moves as a result of the expansion of the heated ionized region. That portion moving towards the generator becomes ionized and therefore advances the arc toward the generator. Therefore the arc can be stopped with a sufficient counter gas flow rate and in fact can be turned about so that the arc flows away from the generator.

In the preceeding reports some consideration was given to high power components. In particular a mode filter in rectangular waveguide with strips of lossy material in the side walls was analyzed for attenuation of the spurious modes. In addition an analysis was also made to evaluate the effectiveness of internal gas flow as a means for cooling high power waveguide systems. The amount of power which can be carried away by atmospheric air in lengths of X band waveguide, 1.5 feet long, is shown in Fig. 5. Because of the relatively low thermal capacity of the gas, it would not be practical to cool individual lengths of waveguide sections much greater than 1.5 feet.

During this interval other work directly related to this program was being carried out under other programs[4],[5]. This work will not be discussed here; however, it contributed to our overall picture of the problems in ultra-high power transmission lines and strongly influenced our decision to develop several high power components for

the TE_{01}^{o} mode in circular waveguide as discussed in this report. For reference purposes, however, the following remarks pertain to why the above high power components were selected for development in circular waveguide.

Careful consideration of the TE_{01}^{o} mode in circular waveguide indicates that the following advantages recommend the circular mode for ultra-high power transmission lines. (The only other mode which warrants attention is the TE_{10} mode in rectangular waveguide; however, once its size is increased to that comparable to circular waveguide then it loses its advantage). The advantages for TE_{01}^{o} waveguide are:

1. The circular mode has the advantage of lowest loss.
2. High peak powers can be handled in the circular waveguide operating in the low loss mode.
3. The low loss coupled with the large surface area allow adequate cooling by radiation and convection.
4. The maximum value of electric field does not occur on the walls so wall imperfection cannot greatly influence breakdown.
5. Because only transverse currents exist in the cylindrical waveguide carrying the TE_{01}^{o} mode, arcing is minimized at poor joints since the current flows parallel to rather than across the joint.
6. The disposition of the wall currents allow a simple technique for mode filtering, since all of the other modes except the TE_{on}^{o} modes will have current components which are axial. Any gaps occurring in a transverse plane do not effect the low

loss mode, but do effect the other modes.

7. The circular cross-section is relatively free from distortion under conditions of pressurization (on the other hand large rectangular waveguide would be very prone to distortion because the surfaces are so large).
8. The circular waveguide from a practical point of view is easy to machine.
9. Because of the high peak power capability, high dielectric strength gas can be avoided in large sections of the transmission line.

There are disadvantages to using circular waveguide in the TE_{01}^{o} mode which are related mainly to the excitation of spurious modes. First, if the power which goes into these modes is simply dissipated in the system, then these losses would wipe out the gains of using the low loss mode in the first place at least with respect to achieving low loss operation. The advantage of handling high peak power levels is not lost however, if proper mode filtering is employed. A second disadvantage to be found in the over-sized waveguide is that spurious modes may experience resonances or come close to cutoff with the result that the field strengths of these modes may become large enough to inititate a discharge and cause a complete failure of the transmission line. Once a discharge has occurred, excessive mode conversion may take place with disastrous results on other components in the transmission line. Finally, a disadvantage may be the large size of the pipe; however, this may only be a laboratory limitation.

Breakdown Near a Hot Surface

One of the problems associated with the improvement of the ultra-high power handling capability of transmission lines and components is the reduction of arcing threshold caused by localized hot spots. This problem is inherent in high powered components. It is not difficult to see how non-thermodynamic equilibrium conditions arise in microwave components because of local dielectric or resistive losses and non-uniform geometry (e.g., microwave windows). The effect of a hot spot is to establish local gas density gradients adjacent to the surface. If the gas adjacent to the hot surface is in thermodynamic equilibrium with surface, the local gas density and temperature are uniform and such cases are handled by ordinary breakdown theory[7]. However, where local heating occurs the non-equilibrium conditions give rise to density gradients and consequently convective currents.

The purpose of this section is to evaluate breakdown in the presence of natural and forced convection currents. These currents, as will be seen, produce an effect greater than would be predicted from just cooling of the hot surface

One of the basic parameters in breakdown is the ratio of electric field to pressure, E/p, because it determines the average energy of the electrons. The pressure enters as a measure of gas density which is the important factor affecting breakdown. The use of pressure for density is common because it is easier to measure pressure than density; however, the actual pressure must be corrected for temperature by

$$p = p_{actual} \frac{T_{standard}}{T} \qquad (2)$$

In the past, breakdown under non-uniform conditions where E/p varied due to electric field gradients has been studied[3]; however, a similar but more involved problem is the case where E/p varies due to gradients in gas density, a problem hitherto largely ignored. This problem was introduced in the preceeding report. In this section direct numerical solutions of the breakdown equation will be discussed. The variational type of solution which was discussed in the preceeding report was not used because the direct approach gave satisfactory results.

Breakdown theory is based on the equation of electron continuity which equates the various rates of electron production and loss. If the rate of electron production exceeds the rate of loss, then we have the possibility of a breakdown occurring. This production process for ordinary breakdown theory is described for most cases by the following electron continuity equation when no density gradient exists

$$\frac{\partial n_e}{\partial t} = \nabla^2 (Dn_e) + \left(\frac{\nu_n}{D}\right) (Dn_e) \; . \qquad (3)$$

The threshold for breakdown occurs when $\partial n_e/\partial t = 0$ (i.e., an

infinitely long time is allowed for the electron density to build up). Thus

$$\nabla^2 \varphi + k^2 \varphi = 0 \qquad (4)$$

where

$$k^2 = \left(\frac{\upsilon_n}{D}\right)$$

and

$$\varphi \doteq Dn_e \ .$$

This is the point at which the electron density barely begins to build up. The quantity k^2 is a function of the breakdown parameter (E/p) and this, in general, is a function of position because of the spatial variation of electric field and p_o. Therefore the solution of Eq. (4) often requires numerical methods. The determination of the breakdown condition actually proceeds by solving Eq. (4) for φ satisfying the boundary conditions and then determining k^2 and finally E_e/p where E_e is the dc equivalent field.

In the vicinity of a hot surface where E may be essentially constant there exists a boundary layer of gas across which the temperature drops from its value at the wall down to that of the

ambient gas. In a constant pressure system, this means that the gas density or p , the pressure equivalent of gas density, is low at the hot surface and increases to a constant value corresponding to the ambient gas temperature away from the hot surface (see Eq. (2)). In the regions of low gas density near the hot surface, net electron production may be high enough to cause a breakdown even though there may be no net production remote from the surface, in the cooler gas. Since k^2 increases with increasing E_e/p this means k^2 is largest at the surface and decreases to a constant value far from the surface where there is no temperature variation and hence no density variation.

In the previous report we attempted a simplified solution of Eq. (4) by assuming k^2 varied exponentially from a large positive value down to a negative value (due to attachment) remote from the surface. Note that the extra term in Eq. (1) has been neglected. The continuity equation was then solved by numerical methods and the results shown in Figs. 1 and 2 of that report. The boundary conditions for this solution were that the quantity $\varphi = Dn$ be zero at the hot surface and approach the solution appropriate for constant coefficients in Eq. (4) a sufficient distance away. These results show a range of small values of p_oL for which the hot surface does not control breakdown. The quantity L is the film thickness and p_o is the remote value of equivalent pressure. We have considered, so far, the problem of a single plate with a film of hot gas adjacent to surface and the electric field uniform at the surface. This model is adequate since the significant values of film thickness will be found to be much smaller

than the spacing between the hot parallel surfaces. In a more accurate model with air flow between two hot surfaces the temperature drops from its value at each surface down to an ambient value in the middle, a boundary layer existing at each surface.

In order to evaluate more accurately the effect of the film of hot gas, a piecewise linear solution of Eq. (1) was tried. We assumed a step change in temperature from the wall to the ambient gas temperature; likewise k^2 changed accordingly in steps over the same interval, being positive within the film and negative in the space between the boundary layers. Fig. 6 illustrates the assumed variation. The solution for φ within the films is a sinusoid and in the region hyperbolic cosine. For a physically acceptable solution, the boundary condition requirements are that the electron density and electron diffusion current be continuous at the film edge; these requirements yield the following breakdown condition

$$\frac{1}{D_o k_o} \cot k_o \left(\frac{d}{2} - L\right) = \frac{1}{D_1 k_1} \tan k_1 L \qquad (5)$$

The subscripts indicate which region the quantities are associated with. The quantity k_o is imaginary in the mid-region, if electron attachment dominates as it does for our purposes, converting the cotangent into a hyperbolic cotangent. The equation above is transcendental and can be solved by graphical methods.

An experimental curve for k as a function of E_e/p in air[7] was used to convert the graphical solutions to a universal breakdown curve whose validity is consistent with our assumptions. When a breakdown criterion such as Eq. (5) is obtained, it is seldom solved directly in such a form. It is customary to normalize the equation with respect to appropriate scaling parameters which enable one to scale solutions to similar geometries with different characteristic dimensions. In this parallel plate model the parameters are E_e/p_o, p_oL, p_od and T_1/T_o. All parallel plate geometries having all these parameters the same are said to be identical. In Fig. 7 there is plotted a normalized solution of the two plate breakdown equation. Here p_od has been chosen very large to approximate the experimental work described later. For the condition that the surfaces and the gas are at temperature T_o, the breakdown threshold value of E_e/p_o is 31.5. If the bulk of the gas rises to the hot wall temperature, E_e/p_o is reduced by the ratio T_o/T_w. Notice that if p_oL can be reduced to below a value of about 3 the threshold is then substantially unaffected by the presence of the hot surface. Flowing air by the plates accomplishes this reduction in p_oL. This model predicts significant reductions in breakdown thresholds, but a more correct continuity equation will have to be solved to substantiate these predictions.

The application of the ordinary continuity equation to breakdown near hot surfaces required simplifying the problem by assuming the existence of two uniform regions. More exactly, because of the spatial variation in ν and D due to gas density gradients, the ordinary

continuity equation becomes modified. The ordinary equation is generally enough to allow for spatial variation of electric field alone but not in gas density. The modified equation which was derived in the preceeding report for the one dimensional case is

$$\frac{\partial}{\partial x}\left(\phi \frac{\partial \psi}{\partial x}\right) + \frac{\nu_n}{D}\phi\psi = 0 \ , \qquad (6)$$

where

$$\psi = \frac{Dn_e}{\phi}$$

$$\phi = \frac{T}{T_o}$$

Here T is a function of position and T_o is the ambient temperature of the gas which in the parallel plane case is the temperature at the mid-point. The variable x is the distance measured normal to the surface. The quantity ϕ embodies the spatial temperature variation; note, if ϕ is a constant, this equation reduces to the ordinary breakdown equation.

Since a reliable theory of film thickness is not available, we assumed an exponential spatial temperature variation. The resulting

form for the parameter ϕ is for the single plate case

$$\phi = \frac{T}{T_o} = 1 + \left(\frac{T_w}{T_o} - 1\right) \quad e^{-x/L} \tag{7a}$$

where

$$0 \leqslant x \leqslant \infty$$

and for two plate case in the right half plane

$$\phi = \frac{T}{T_o} = \frac{T_w}{T_o} - \frac{(T_w/T_o - 1)}{1-e^{-d/2L}} \left[1-e^{-(d/2 - x)/L}\right]. \tag{7b}$$

where

$$0 \leqslant x \leqslant d/2 \ .$$

The quantity L is a decay constant with the dimensions of distance and is interpreted as the nominal film thickness.

A digital computer solution for the single plate problem was undertaken using the modified continuity equation, Eq. (6). The boundary conditions however, are the same as those used for the approximate solution. There are two methods of solution - one involves the

variational approach described in the previous report and the other the direct numerical solution. For the one dimensional case the latter is the simpler and more straightforward. Only the one plate problem was set up for the solution because under most experimental conditions it was anticipated that the gap distance would be much larger than the film thickness and so the results would apply to the two plate case also. Fig. 8 shows the results of the computer solution for single plate problems. The values of p_oL where E_e/p_o begins to drop are in the same range as predicted by the approximate piecewise linear solution of the two plate problem (for $p_od \to \infty$) Fig. 7; however, the range of p_oL over which the transition occurs to breakdown controlled by the hot surface is significantly greater. This is due to extra term in the continuity equation and the more gradual change in temperature in the film.

Numerical solutions for the spatial variation of $\psi = Dn_e/\phi$ was obtained as part of the overall solution for breakdown. Since both D and ϕ do not vary widely, the function φ is a fair indication of the electron density distribution during the initial stages of breakdown. The form of the function φ does not change with time, only the amplitude. Several cases showing how φ peaks near the hot surface (S = 0) are given in Fig. 9. The curves clearly illustrate that as the remote value of E_e/p_o becomes smaller (i.e., the bulk of the gas becomes exposed to ionization rates further below the threshold for breakdown), the electron density becomes more highly localized at the hot surface.

The theoretical analysis shows that breakdown near a hot surface is strongly dependent upon the size of the boundary layer of hot gas. If it is infinitely thin, we expect no reduction of the breakdown level of the system due to the hot surface. Since one can vary film thickness by flowing air past the surface (the faster the flow the smaller the boundary layer), it is conceivable that a sufficiently rapid flow past a hot surface would inhibit the breakdown even if the temperature of the surface is unaffected. In order to predict the effect of gas temperature gradients, some knowledge of the film thickness is required.

A derivation for film thickness can be based on the following considerations: If we have an air stream past a hot surface, the velocity of the stream is zero at the surface and rises to free stream velocity away from the surface; this velocity variation arises from the viscous forces. Hence the energy carried away from the surface is transmitted to the gas immediately adjacent to the surface by conduction; no convective transport is possible at the surface because there is no bulk movement of air immediately adjacent to surface. The heat conducted away from the boundary of the hot surface must equal the heat transported away by convection in the film; this equality is expressed by the equation for continuity of energy flow,

$$-k \left(\frac{\partial T}{\partial x} \right)_w A = h \, (T_w - T_o) \, A \, , \qquad (8)$$

where k is the thermal conductivity of air, h is the convective heat transfer coefficient and the subscript w denotes evaluation at the hot surface. From Eq. (8) the ratio k/h is

$$\frac{k}{h} = \frac{T_w - T_o}{(\partial T/\partial x)_w} \quad . \tag{9}$$

Note that k/h has dimensions of length which may be related to film thickness. For example, substituting an exponential form for T, Eq. (7a) into Eq. (9), the interesting result is

$$L = k/h \quad , \tag{10}$$

k/h is essentially the film thickness.

This discussion is complicated by the fact that h is a function of the distance along the hot surface in the direction of gas flow. A simple theoretical result that can be obtained is[8]

$$h_y = 0.332 \, N_p^{1/3} \, k \sqrt{\frac{u_\infty}{\nu y}} \quad , \tag{11}$$

where y is distance measured from the leading edge of the hot surface, the quantity N_p is the dimensionless Prandtl number of the gas, ν is the kinematic viscosity term and u_∞ is the free stream velocity.

From Eq. (11) we obtain an equation for L

$$L = \frac{1}{0.332\ N_p^{1/3}} \sqrt{\frac{\nu y}{u_\infty}} \qquad (12)$$

The quantity u_∞ is difficult to calculate for complicated geometries and non-uniform flows. An order of magnitude calculation shows that this thickness is 0.5 mm for the maximum flow conditions in the experimental work on the hot flat surface. For reference $\nu = 0.150$ cm^2/sec for air, $N_p = .68$ and in the particular calculation $y = 2$ cm and $u_\infty = 1240^*$ cm/second.

Experiments were undertaken to evaluate the importance of boundary layer effects. In general the object of these experiments was to measure the breakdown power as a function of film thickness (by changes in the air flow past the hot surface) and the temperature ratio between the hot surface and the cooler gas.

Since a resonant TM_{010} cavity with a narrow height provides an approximate parallel plate geometry, which is relatively simple to analyze, one was used in a set of experiments. The cavity was heated and pre-cooled air was forced through it as illustrated in Fig. 10. Pertinent dimensions are shown in Fig. 10 as well as the air flow pattern parallel to the flat surfaces. The purpose of pre-cooling the air was to partially counteract the initial heating of the gas as it entered through a small hole in the cavity wall. The microwave circuit arrangement is illustrated in Fig. 11. The power was varied

*Nominal area (Fig. 10) 0.09 in^2 and maximum flow of 92 cfh.

(by the power divider) slowly to the point of breakdown which was determined by the distortion of the pulse transmitted through the cavity. The cavity was checked before each measurement to make sure that it was operating at its resonant frequency to offset any drifting. Cavity temperature was monitored with a thermocouple mounted outside the resonant cavity but near the center of one of the flat surfaces. The air was pre-cooled by passing it through a coil in a dry ice alcohol bath.

A simple preliminary experiment indicated that the percentage change in the air pressure of the cavity over that of atmospheric pressure was negligibly small. It would be difficult to measure gas temperature while conducting the experiment because of the disturbance produced in the cavity by a temperature probe. Temperature calibration experiments were conducted before the breakdown experiments by placing a thermocouple into the center of the cavity to monitor the gas temperature while simultaneously monitoring wall temperature with the thermocouple mounted on the top wall. Figure 12 shows some of the results of the calibration experiments. Note that we were basically limited in our attempt to obtain small ratios between the gas and the wall temperature and that such ratios eventually became constant with respect to flow rate.

The breakdown measurements were taken in the following fashion: As the cavity was heated the change of breakdown power with temperature was monitored; when the temperature finally stabilized, the air flow was introduced and then breakdown power values were recorded

as a function of wall temperature and flow rate. Thus it was possible to compare breakdown values with and without flow for the same wall temperature. To aid in interpreting the experimental results recall that the electron continuity equation governing the case where gas density gradients are present would reduce to the ordinary continuity equation if ϕ equalled a constant. There are two possibilities for this occurring: 1) where the gas has come into thermal equilibrium with the hot surface and 2) where the film thickness is so small that, in spite of the hot surface, the gas is uniformly at a lower temperature than the surface. The latter condition occurs when flow rates are very high. Now suppose we have a cavity at some uniform temperature under zero flow conditions; then breakdown would be predicted by ordinary theory since there is no temperature gradient. As we introduce flow we produce a temperature gradient, and we expect a greater breakdown power than in the case of the cavity operating uniformly at the wall temperature. This occurs because the center of the cavity is cooler implying a greater gas density in the middle and therefore a smaller or even negative contribution to the total electron production. As the flow rate increases further, the film thickness decreases until it is so small that we approach, essentially, uniform conditions and breakdown is again predicted by the ordinary theory but with the bulk of the gas in the cavity now at some temperature lower than that of the hot walls.

Ordinary breakdown theory for uniform fields predicts that at normal pressures the breakdown power is related to pressure

by $$P = cp^2 \tag{13}$$

Here c is a proportionality constant and p is the pressure equivalent of density. We will calculate p corresponding to the gas in equilibrium with the hot surface using the perfect gas law from

$$p = p_r \left(\frac{T_r}{T_o}\right). \tag{14}$$

where the subscript r indicates a reference value and T_o is the gas temperature. This expression substituted into the preceeding equation results in (for $T_o = T_w$ in equilibrium)

$$PT_o^2 = cp_r^2 T_r^2 = \text{constant} \tag{15}$$

which simply points out that, in equilibrium, the product of breakdown power and cavity wall temperature squared remains constant as the wall temperature is varied. As equilibrium is destroyed by increasing gas flow the experimental values of PT_w^2 should rise above this value if the breakdown is affected by the boundary layer as predicted above. Plotting the results in this fashion factors out the changes in breakdown threshold due to changes in wall temperature

alone and any increase above the reference can be interpreted as being due to the gas density gradients alone. As flow rates become large the boundary layer becomes important; breakdown is then controlled by the ambient gas temperature, T_o, and the plot of PT_w^2 versus flow rate should approach a new reference level

$$PT_w^2 = (cp_r^2 T_r^2) \left(\frac{T_w}{T_o}\right)^2 \qquad (16)$$

Experimental results plotted in this manner are shown in Figs. 13 and 14 in terms of PT_w^2 and gas flow where PT_w^2 is normalized to a value of unity for zero flow. Two initial wall temperatures are shown. The flow rate is in cubic feet per hour. The results, in general, exhibit the predicted behavior at medium rates of flow - there is significant increase above the dashed reference line. However, final levels reached by the experimental value of PT_w^2 fall short of the upper limit calculated using Eq. (16). Additional sets of data, not shown, demonstrated a downward trend at high flow rates. Although some scattering of the data is evident and the upper limits not reached, nevertheless the experiments exhibit a significant increase in the quantity PT_w^2 which is too large to be explained by experimental error. Figure 15 shows that PT_w^2 is relatively constant for zero flow but some increase is evident. The 10% increase might be due to the presence of natural convective currents or possibly due to the cavity Q dropping somewhat at high temperatures. When the

gas is forced through the cavity and there is no temperature difference between the stream and the cavity there is no effect on the breakdown threshold. This means that it is the effect of flowing cool air that raises the breakdown threshold and not mere air movement alone.

A second experiment was conducted to obtain qualitative confirmation of the theory with a useful geometric configuration which unfortunately becomes difficult to analyze. In this experiment a wire filament was stretched across the cavity parallel to the two flat faces, transverse to the direction of propagation and passing through the region of maximum E field. The wire tends to increase the local electric fields and so the cavity has a lower breakdown threshold under normal conditions. The wire filament was heated by passing current through it as shown in Fig. 16. In this experiment, then, the filament not only alters the local fields but also alters the local gas density as its temperature is varied. The object in this experiment is to determine the extent to which air flow past the wire changes the breakdown threshold. We reasoned that for the same filament temperature, the breakdown power required at high flow rates would be larger than that for low flow rates because of the reduction in the size of the heated gas layer. This controlled experiment is valuable because it simulates a small foreign body becoming heated under high average power conditions (Fig. 2).

The microwave circuit arrangement in this experiment is the same as before except that room temperature air is fed in at the bend,

(Fig. 16) passes through the input iris and across the wire filament. The wire used was platinum-rhodium of diameter five thousandths. The temperature of the filament was monitored by measuring its change of electrical resistance and using tables of relative resistance versus temperature found in the American Institute of Physics Handbook. The experimental procedure involved fixing the gas flow rate and changing the current carried by the wire. At each value of current the resistance and breakdown power (in the presence of a radio active source) were determined.

The resulting measurements of breakdown power versus temperature for a number of gas flow rates are shown in Fig. 17. For several small values of flow rate the points fall on roughly the same breakdown curve. The important observation is that after a certain temperature has been reached the breakdown threshold begins to fall rapidly with further increases in temperature. At the maximum flow rate (15 units) the curve breaks at a higher value of temperature and the points are higher than those for small values of flow. Again we interpret the difference between flow rates as being due to differences in film thickness. Hence, a smaller region of high electron production implies greater electron diffusion losses and therefore higher thresholds for breakdown. Some insight into these results can be gained by reference to the earlier analysis, Fig. 8. The theoretical solutions predict that the reduction in the breakdown threshold begins when p_oL exceed about 1 (mm Hg-cm) for high temperature ratios. Since these experiments are conducted at atmospheric pressure, this means that the film thickness should

exceed approximately 1×10^{-3} cm and suggests that the heated wire may be treated as a flat surface. The breakdown measurements in Fig. 17 indicate that quite high temperatures must be reached, 700°C, before the film thickness becomes large enough to reduce the breakdown threshold.* Even for zero flow natural convection must be effective in cooling the air adjacent to fine heated wire suggesting that small foreign particles must reach temperatures in excess of a 1000°C in order to initiate failures in a waveguide system. Although in these preliminary experiments with a hot wire the values of some of the pertinent variables are not accurately known, the increase in breakdown threshold with gas flow rate is significant as is the threshold in temperature where the breakdown power begins to decrease.

From the experiments and theory, Fig. 8, we conclude that the theory is useful in indicating the factors controlling breakdown at a hot surface. The hot wire experiments showed that values of p_oL of the order of unity were involved while the hot cavity experiments indicated values of the order of 100. Thus both ends of the transition region, Fig. 8, were explored.

Components for Ultra-High Power Levels

Several components for ultra-high power levels were to be designed for this program. Based upon the arguments reviewed in the first section it was recommended that a transducer and mode filter for circular waveguide carrying the low loss mode (TE_{01}^{o}) be developed. These components would be the first required in the development of a

*Thermionic emission is an unimportant factor for the conditions of these experiments.

complete transmission line, particularly in connection with evaluating subsequent components.

In a high power transmission line, choosing a waveguide diameter involves considerations such as breakdown power, waveguide temperature rise, the spurious modes that can be allowed and the attenuation to the desired mode. Since the transmission line has as its design goal an average power level of 100 kilowatts, the temperature rise of the waveguide wall will be extremely high unless a large diameter is chosen so that water cooling will not be necessary. It has been determined[4] that a circular waveguide (TE_{01}^{o} mode) with an inner diameter of 3.00 inches will have a temperature rise of approximately 55°C at this power level. Also the breakdown power for this size waveguide, determined from the universal breakdown curves[4], is approximately 12 megawatts. Since the peak power requirement for this program is 5 megawatts, the 3.00 inch diameter copper waveguide would certainly be adequate. The diameter of 3.00 inches is also such that the TE_{02}^{o} mode would be below cutoff in the frequency range of 7.5 - 8.4 Gc. The actual cutoff for the TE_{02}^{o} mode is 4.5% above the high frequency end of 8400 mc/s. The total number of modes that are above cutoff in this frequency range is 13. Preventing the propagation of the TE_{02}^{o} mode is desirable since this mode does not readily lend itself to filtering. The attenuation of a circular waveguide of 3.00 inch diameter to the TE_{01}^{o} mode would be 0.0064 db/meter[4] in this frequency range. This is indeed an extremely low loss compared to WR 112 which is 0.102 db/meter. This is an inherent advantage to the TE_{01}^{o} mode in circular waveguide.

Since both low power and high power test equipment was available in a higher frequency range, 8.6 - 9.6 Gc, at Microwave Associates, it was decided to build a scaled model in this range so that complete evaluation would be possible. When evaluation was complete a final model based on the scaled model would be constructed. The circular waveguide size was scaled from 3.00 inch diameter to a 2.63 inch diameter by maintaining the same ratio of free space wavelength to cut-off wavelength in the two models,

$$\frac{\lambda_o}{\lambda_{co}} = \frac{\lambda'_o}{\lambda'_{co}} \tag{17}$$

where the primed quantities refer to the scaled model. This choice of dimensions insures that at the scaled frequency there will be the same phase velocity, wave impedance and ratio of guide wavelength to free space wavelength. The number of modes propagated in the smaller guide will also be identical to the larger size waveguide. Although a waveguide diameter of 2.63 inches would be required, the closest commercially available size is 2.62 inches, which is close enough for our purposes.

The alignment of two mating sections of circular waveguide is very critical since any misalignment can launch spurious modes. This alignment problem can be minimized by the use of a joint as shown in Fig. 18. The joint is simple to construct and provides excellent alignment of the two mating waveguides. Even though the desired mode

does not require good contact at the joints, the spurious mode power can become great enough to cause arcing under unfavorable conditions. As will be seen later the mode purity of the mode transducer is nominally 20 db which at the design power levels means a spurious mode power of 1000 watts average and 50 kilowatts peak. Even at this level of power in the spurious mode arcing can be a problem. Since the transducer will require pressurization, an O-ring groove has been provided in the male flange. The rubber O-ring is a silicone rubber base impregnated with carbon to make it lossy in order to cut down any leakage at the joints.

In considering the type of transducer to be built various types were considered which might be adapted for high power operation. Gradual developments such as those suggested by Southworth[9] and P. Marie[10] are too long and cumbersome. Several more compact types which have been recently described[11,12,13] also lack the physical characteristics of a short transducer that might even be incorporated into the vacuum envelope of a high power tube so that peak power failure problems are removed and water cooling would be available. A type of transducer developed at Microwave Associates[14] does have these characteristics if its bandwidth could be increased. A sketch of the transducer is shown in Fig. 19. It was felt that stronger coupling by means of larger slots would increase the bandwidth and incidentally improve the power handling capability of the device. The dimensions of the scaled transducer are given in Table 1.

The principle of operation of the transducer is as follows:

The transition consists of four resonant slots and a feed section. The feed section is made up of a quarter wavelength impedance transformer, a bifurcation and two short circuits. The impedance transformer is necessary since the actual design results in a rectangular waveguide input different from the actual external mating waveguide, WR 112. The bifurcated waveguide acts as a power splitter so that half the power is available to couple out of the top and bottom coupling slots. The purpose of the shorting plates is to insure total coupling through the slots. The resonant slots are oriented 45° with respect to the rectangular waveguide axis so that the electric field excited in the slots coincides with the maximum electric field found in the TE_{01}° mode in the circular waveguide output section. The resonant slots are also positioned $\lambda_g/2$ apart in the rectangular waveguide so that excitation of the slots is always 180° out of phase. The diameter of the circular waveguide at the transducer output is adjusted so that the maximum electric field excited in the slots coincided exactly with the maximum electric field for the TE_{01}° mode which lies on a diameter $d = 0.48\ D$, where d is the diameter of the maximum electric field and D is the diameter of the circular waveguide.

The initial results with the increased slot size and circular waveguide diameter were very poor since typical values of mode purity were 8 db and VSWR was nominally 3.0 from 8600 to 9600 mc/s. On the supposition that an impedance mismatch existed between the coupling slots and the circular waveguide and further that the larger circular waveguide size allowed additional spurious modes, a circular ring was

made up. The inside diameter was that which would have been obtained if the earlier model[14] diameter had been used. The ring was made $\lambda_g/2$ long and positioned for maximum bandwidth and VSWR. The resulting VSWR bandwidth and mode purity are plotted in Fig. 20. The bandwidth is 8.3%* for a VSWR <1.3 and is centered at a frequency of 8.8 Gc. The insertion loss is 0.1 db. The mode purity is greater than 20 db over most of the same frequency range except for a small region at the upper end of the band. Mode purity was measured with the same technique used by Lanciani[14]. This method consists of sampling the amplitude of spurious modes at the waveguide wall with a rotary sampler which does not couple to the TE_{01}^{o} mode and comparing the largest value to that of a pure TE_{11} wave of known power. The mode purity is given by

$$MP = 10 \log P_{11}/P_s \ , \quad \text{(db)} \tag{18}$$

where P_{11} is the maximum sampled power from a reference TE_{11}^{o} mode at the same power level as the line power and P_s is the maximum sampled power from the spurious modes.

High power tests were run on the scaled version of the mode transducer in order to determine its power handling capability. The extremely high power was simulated in a cavity formed by placing a moving short in a section of the circular waveguide and an iris at the input rectangular waveguide. A plot of equivalent peak power in megawatts as a function of air pressure in psia gives the results in

*The bandwidth for the final model was 8.4% (See Fig 29).

Fig. 21. The short circuit in the cavity was varied so that the voltage maximum was moved in the cavity to obtain the weakest point. A typical case, not the worst, in Fig. 21 is curve II. Since breakdown power is proportional to the square of the absolute pressure in this pressure range and if arcing joints and other failure mechanisms do not come into play, the data should fall on a straight line with a slope of 2. The line may be extrapolated to atmospheric pressure where a breakdown power of 1.5 megawatts is obtained. The worst case and its extrapolation to atmospheric pressure is shown as curve I - a breakdown power of 390 kilowatts is obtained at one atmosphere. It was observed that the breakdown in the worst case was occurring at the coupling iris of the transducer. It was also observed that the transducer and input rectangular waveguide ran hot to the touch while the circular waveguide was running with no noticeable rise in temperature.

The conditions for testing were: pulse width 1.0 microsecond, pulse repetition rate 1000, input power (not in the cavity) nominally 120 kw peak and 120 watts average, test frequency 8800 - 9000 mc/s. The reason for the spread in frequency is that for various positions of the short circuit, the frequency had to be re-adjusted to keep the cavity in resonance. It can also be seen from Fig. 21, curve I, that air at a pressure of 54 psia would be required to handle 5 megawatts peak power. The final design at the lower frequency should of course handle the 5 megawatts at a lower pressure because of its larger size. As alternatives a high dielectric strength gas at lower pressure could be used or consideration could be given to incorporating the transition

into the vacuum envelope of the tube.

The final transducer with a goal of 7.5 to 8.6 Gc for an operating range is a direct scaling of the above model (8.6 - 9.6 Gc). The final model is made completely from OFHC copper and is hard brazed in order to be able to handle the extremely high average power. A photograph showing an exploded view and listing of all the parts is shown in Fig. 22. The transducer is water cooled by means of longitudinal channels in the sides located close to the areas of high heat concentration. The cooling channels are to be fed in parallel for maximum possible cooling and the fittings are standard 3/8" flare tube fittings. Helicoils will be employed for the screws at the rectangular waveguide input end since the copper will be extremely soft after furnace brazing. From the insertion loss data on the scaled version approximately 2 kilowatts will be dissipated by the transducer. A second photograph of the transducer partially assembled is shown in Fig. 23. This figure shows the water cooling channels in better detail as well as the coupling plate and bifurcation.

As a second component a mode filter or suppressor was designed and constructed. In an ultra high power transmission spurious modes can be launched by discontinuities such as bumps in the waveguide walls, eccentricity of the transmission line, mode transducers, tapers and many more. In general, this spurious power will be distributed among several modes in a multimode transmission line. For the case under consideration the spurious power level might be, nominally, 50 kilowatts peak and 1000 watts average. In a typical system the transmission

line will consist of a mode transducer, components and a feed horn or antenna. Since the spurious modes will not readily pass through the mode transducer and may be reflected from the components and feed horn, the resulting high standing waves could produce breakdown in the waveguide or excessive heating. It is important therefore that some thought be given to the desired characteristics of a mode filter, which must attenuate all of the spurious modes.

For simplicity assume that the spurious power is contained in a single mode. It is then possible to analyze the mode transducer as a three port junction where for definiteness port number 1 represents the $TE_{10}^{\square}$ rectangular input, port number 2 represents the coupling to spurious mode arm which can be resonant and port number 3 represents the TE_{01}° circular waveguide output. To point out the worst case, the general three port lossless junction has the property that a short circuit suitably located in one arm entirely decouples the other two arms from each other resulting in total reflection in the input arm. Therefore, even for weak excitation of the spurious mode, if it happens that the energy transferred to that mode is reflected back without loss toward the junction in the worst phase, then there will be no transfer of energy to the desired mode and everything will be reflected at the input port.

From standard circuit analysis it can be shown in matrix notation that the amplitudes of the waves entering the lossless three port junction in terms of the waves leaving the junction is

$$\begin{bmatrix} (1-S_{11}\rho_1) & -S_{12}\rho_2 & -S_{13}\rho_3 \\ -S_{21}\rho_1 & (1-S_{22}\rho_2) & -S_{23}\rho_3 \\ -S_{31}\rho_1 & -S_{32}\rho_2 & (1-S_{33}\rho_3) \end{bmatrix} \begin{bmatrix} E_1 \\ E_2 \\ E_3 \end{bmatrix} = \begin{bmatrix} S_{11} & E_{01} \\ S_{21} & E_{01} \\ S_{31} & E_{01} \end{bmatrix} \qquad (19)$$

where S_{mn}, m, n = 1, 2, 3 are the scattering coefficients of the junction; E_1, E_2 and E_3 are the amplitudes of the waves traveling away from the junction; E_{01} is the amplitude of the wave incident at port number 1; and ρ_1, ρ_2 and ρ_3 are the reflection coefficients at the reference planes looking back out of the respective ports. By reciprocity $S_{12} = S_{21}$, $S_{13} = S_{31}$ and $S_{23} = S_{32}$. The above matrix equation can be written in algebraic form and making the above substitution

$$(1-S_{11}\rho_1)\, E_1 - S_{12}\rho_2 E_2 - S_{13}\rho_3 E_3 = S_{11} E_{01} , \qquad (20)$$

$$-S_{12}\rho_1 E_1 + (1-S_{22}\rho_2)\, E_2 - S_{23}\rho_3 E_3 = S_{12} E_{01} , \qquad (21)$$

$$-S_{13}\rho_1 E_1 - S_{23}\rho_2 E_2 + (1-S_{33}\rho_3)\, E_3 = S_{13} E_{01} . \qquad (22)$$

Since ports (1) and (3) can be considered as terminated in matched loads (i.e., $\rho_1 = \rho_2 = 0$), the solutions for the output wave amplitudes are

$$\frac{E_1}{E_{01}} = \left[S_{11} + \frac{S_{12}^2 \rho_2}{1 - S_{22} \rho_2} \right] \tag{23}$$

$$\frac{E_2}{E_{01}} = \frac{S_{12}}{1 - S_{22} \rho_2} \tag{24}$$

$$\frac{E_3}{E_{01}} = \left[S_{13} + \frac{S_{12} S_{23}}{(1 - S_{22} \rho_2)} \right] \tag{25}$$

In order to evaluate the scattering coefficients the unitary property can be used

$$[S][S^*] = [I] \tag{26}$$

since the junction itself can be assumed lossless. The asterisk denotes conjugate and $[I]$ is the unity matrix. Also since S_{12} represents the coupling to the spurious mode arm, it is most useful to solve for the scattering coefficients in terms of S_{12}. In order to obtain an instructive solution and solve for the coefficients it is necessary to make several simplifying assumptions:

1) For a well matched transducer $|S_{11}| \ll 1$ and $|S_{33}| = 0$
2) S_{11}, S_{22} are both real and positive by proper choice of reference planes.

With the above assumptions it is possible to solve the algebraic equations obtained from the unitary property for the scattering coefficients in terms of S_{12} where S_{12} also is real to give

$$S_{11} = \frac{S_{12}^2}{\sqrt{1-2S_{12}^2}} \quad , \tag{27}$$

$$S_{22} = \sqrt{1-2S_{12}^2} \quad . \tag{28}$$

$$S_{13} = \sqrt{1-S_{12}^2} \quad , \tag{29}$$

$$S_{23} = -S_{12} \quad . \tag{30}$$

The results from the above equations can be substituted into Equations (23), (24) and (25) which upon simplification become

$$\frac{E_1}{E_{01}} = \frac{S_{12}^2}{\sqrt{1-2S_{12}^2} - \rho_2(1-2S_{12}^2)} \tag{31}$$

$$\frac{E_2}{E_{01}} = \frac{S_{12}}{1-\rho_2\sqrt{1-2S_{12}^2}} \tag{32}$$

$$\frac{E_3}{E_{01}} = \sqrt{1-S_{12}^2} - \frac{\rho_3 S_{12}^2}{1-\rho_2\sqrt{1-2S_{12}^2}} \tag{33}$$

The three equations above describe the mode transducer behavior as a function of the coupling to the spurious mode and the reflection coefficient at the output of port number 2. It should be remarked that the analysis has been organized to bring out the effect of a resonance in the equivalent line for the spurious mode. In general

$$\rho_2 = |\rho_2| \, \epsilon^{2\alpha z} \, \epsilon^{j2\beta z} \tag{34}$$

where ρ_2 is the reflection coefficient terminating port number 2, α is the attenuation per unit length in arm number 2, z is the distance from the reference plane to the termination and β is the phase constant.

If arm 2 is terminated in a short circuit and adjusted for the worst possible reflection in arm number 1 (i.e., $\rho_2 = 1$), it can be seen that Equation (31) approaches a value of unity for $S_{12} \ll 1$, which means an open circuit and total reflection. On the other hand, as the losses in arm number 2 increase the reflection at port number 1 decreases. To show this quantitatively the reflection at the input port is shown in Fig. 24 for varying loss in arm number 2 for three typical values of coupling S_{12}^2. These curves also show the relative transmitted power in the desired TE_{01}^{o} mode. As the coupling to the spurious mode decreases (increasing values of db) the loss required to insure good transmission and low input reflection decreases rapidly.

The results in Fig. 24 may be applied to the mode transducer

built for this program which has a mode purity of 20 db. If there were no losses associated with a resonance of a spurious mode, then from the curves the VSWR would be infinity and the transmission would be zero. If the one way loss in the resonator were only 1.0 db, then the worst possible VSWR would be approximately 1.10 and the transmission would be approximately 90%.

It is also important to observe what is happening in arm number 2, the equivalent resonator for the spurious mode. In the worst case, at resonance for a spurious mode, the values of electric field at the maxima of the standing wave pattern can cause breakdown of the waveguide. The power gain for determining the breakdown threshold relative to the line power is shown as a function of the coupling to the spurious mode and the loss in the resonant section of waveguide in Fig. 25 and in Fig. 26 on an expanded scale. A gain of unity indicates that the maximum value of field strength is equivalent to that corresponding to the power in the main mode. These calculations do not take into account the geometric differences between the various modes and so the values are only approximate. In cases of practical interest a loss of several db is sufficient to reduce the power gain to values below unity. It may be noted that with decreasing coupling (higher values in db) to spurious modes that the gain decreases more rapidly with increasing loss. This means that high mode purity is desirable in a system since it decreases the required loading by the mode filter. These curves, Figs. 25 and 26 should be of significant value to the systems design engineer since they give insight into the amount of

attenuation required of a mode filter and therefore allow some economy in the design. Aside from the enhanced field strengths due to spurious mode resonances, the total amount of power which must be dissipated by the mode filter at resonance is another consideration. From Equation (32) the absorbed power in the resonant mode can be calculated. In Fig. 27 the power dissipated relative to the line power is shown as a function of loss in the resonant section and coupling. Since the model is a three port junction, 1/2 the line power is coupled into the mode filter for the least favorable choice of mode filter loss. This would indeed be a catastrophe. Reference to Fig. 27 shows, however, that close to the minimum amount of power is coupled to the mode filter for loss of 5 db or more. The results given in Fig. 27, as did those in Figs. 25 and 26, show that a certain amount of economy can be achieved in mode filter design by limiting the attenuation to a one way loss of 5 db. This is important for high power mode filters because of the cost of high temperature load material and the machining required for hermetically sealed joints. In any event compactness is always a desirable physical characteristic.

The approach in this program has been different than that used in communication systems where the important factor is the removal of spurious modes so that over long lengths of line distortion of information is minimized. For super power applications, in view of the preceeding analysis, the important factor is to introduce enough attenuation to insure that the spurious mode does not cause a failure or excessive heating at resonance.

The high power mode filter sketched in Fig. 28 was designed and constructed. It consists of alternate conducting rings and lossy rings. This type of filtering has maximum effect on the spurious modes and little or no effect on the TE_{01}^{o} mode. This is due to the fact that all the spurious modes that can propagate in this waveguide have longitudinal currents whereas the TE_{01}^{o} mode has only transverse currents. Thus the conducting wall can be broken without adversely affecting the TE_{01}^{o} propagation, provided the gap remains small with respect to a wavelength. In practice, high temperature load material does not present a matched load, therefore a range of impedances can be presented at the boundary by the choice of the distance to the load material and the gap spacing. In the mode filter constructed a distance of $\lambda/4$ and a gap of $0.1\ \lambda$ was selected. The general configuration of the filter, shown in Fig. 28 includes two sections of lossy material.

In the scaled model as well as the final design the lossy material was placed $\lambda g/4$ back from the inside diameter of the waveguide to increase the coupling of the spurious modes to the lossy material. Since the lossy material has a low impedance, an impedance closer to that of the main waveguide mode, occurs at the gap with this spacing. Placing the lossy material as much as $\lambda g/4$ from the gap also has the desirable effect of further decreasing the coupling to the TE_{01}^{o} mode. The material used was an epoxy-base lossy material called "Custom Load 4101" (Custom Materials Inc.) with our attenuation of 60 db/inch and a dielectric constant of approximately 17. This material does not have a high temperature capability and was used only for evaluation of the scaled version.

The scaled version of the mode filter was constructed for testing at 9 Gc. The loss characteristics for spurious modes were evaluated, using the TE_{11}° mode. The $TE_{10}^{\square}$ - TE_{11}° transducer was readily available from the apparatus used for evaluating the mode purity of the transducer for the low loss mode. The low loss mode transducer was found to have a strong spurious component in the TE_{11}° mode so evaluating the mode filter with this mode would be useful. In order to decrease reflections from the main mode, the transverse slots were separated by a distance of $\lambda/4$.

The two section mode filter, Fig. 28, was considered as a representative element of a complete filter which would give the desired suppression of spurious modes. The nominal $\lambda/4$ spacing between the two slots is also optimum with respect to all possible positions of the standing wave pattern for the spurious modes. The strongest coupling to the lossy material occurs when a current maximum falls at one of the two slots and the weakest when the current maximum falls mid-way between them. Thus there is always a position where some coupling to the lossy material occurs. The mode filter was placed in a section of circular waveguide terminated in a movable short circuit at one end and the TE_{11}° transducer at the other. The standing wave ratio looking into the transducer for various positions of the movable short circuit thus gives an indication of the effectiveness of the filter. For example, the equivalent reflection coefficient can be substituted into Equations 31, 32 and 33 as ρ_2 to predict the performance of the low loss mode transducer. The minimum and maximum VSWR

with respect to position of the short circuit was found to be 8.0 and 32 respectively. The corresponding equivalent one way attenuation is 1.1db and 0.3db. Since, as was pointed out in connection with Fig. 27, a practical minimum value of 5 db attenuation is required; additional two section filters would be necessary in a single section of transmission line in which resonances of spurious modes are possible.

A graphical presentation of the effectiveness of the two section mode filter is shown in Fig. 30. The oscilloscope traces are the reflected signals, as the frequency is swept across the band, from the low loss mode transducer (TE_{01}°) terminated in a length of circular waveguide containing a movable short circuit. The upper trace, Fig. 30a, shows a number of sharp resonances each corresponding to a spurious mode in the absence of the mode filter. The wavy portion of the trace is due to the characteristics of the sweep signal generator. The position of the short circuit affects the position of the resonances. The lower traces, Fig. 30b, show the effect of the mode filter for both a favorable and an unfavorable position of the short circuit. The unfavorable position of the short circuit (i.e., the standing wave) indicates the need for additional filter sections.

A brief experiment to increase the coupling to the two section mode filter was carried out with a short ceramic cylinder which was placed in the mode filter. The coupling appeared to be increased; however, since the dimensions of the cylinder were not precise, there was some question as to whether the improvement was due only to asymmetries. Unfortunately there was no time to pursue this further; but

it is felt that this approach holds promise for a short but effective mode filter.

The scaled model of the mode filter was tested at high power levels along with the $TE_{10}^{\square}$ to TE_{01}° mode transducer in the resonant structure to simulate the high power levels. The mode filter showed no signs of breaking down or of excessive heating due to spurious mode resonances. Therefore, it is expected that the mode filter can handle power levels approaching that of the uninterrupted smooth circular waveguide as was mentioned at the beginning of the report.

The parts of the high power two section mode filter are shown in Fig. 31. The metal parts are made of copper to minimizes losses to the main mode and to maximize heat transfer to the water cooling channels. The end plates are waveguide flanges described earlier. The radial grooves were added to allow easy passage of gas to the back side of the rings; however, the "O" rings (silicone rubber) prevent gas leakage from the waveguide system. The lossy material is Eccosorb MF 500F117 (made by Emerson Cumming). It can withstand 500°F and has an attenuation of 23 db per cm. Originally a loaded beryllium oxide was considered because of its extremely high thermal conductivity and its ability to withstand very high temperatures; however, because of cost and delivery it was decided not to use it at this time.

The bandpass characteristics of the high power mode transducer is shown in Fig. 29. The bandwidth is greater than 8 percent at a VSWR of 1.3 which represents a considerable improvement over the 5 to 6 percent found in the earlier models. The final improvement was

accomplished with a short cylinder (0.375 x 0.625 inches) with a rounded end placed at the center of the coupling plate. Our efforts in extending the bandwidth of this very compact transducer suggests that the 8 percent bandwidth is still not the maximum bandwidth and that further development along the lines carried out in this program would result in bandwidths of perhaps 11 or 12 percent at low values of VSWR.

The design goal for the components was 5 megawatts of peak power and 100 kilowatts of average power. The most critical requirement is the value of peak power in that the input rectangular waveguide itself can only carry about 1 megawatt at atmospheric pressure and therefore pressurization to the level indicated was required. The average power requirement simply dictates that good heat transfer be provided to the cooling surfaces and that the coolant have adequate capacity. For the transducer the loss measurements indicate that about 2 kilowatts will have to be carried away by the coolant. For a 50°C temperature rise of water a flow rate of only 0.2 gallons per minute is sufficient. Examination of Figures 22 and 23 shows a set of parallel independent water cooling channels running the entire length of the transducer. These readily allow more than the required flow rate. The most critical regions are the coupling plate (item 6 in Figure 22) and the tip of the septum (item 9); however, since they are made of thick copper and hard brazed to the sections containing the water channels, adequate heat flow is provided for. Similarly the mode filter section was designed to dissipate several kilowatts. When the

transducer is inserted into a transmission line, exceptional care is required with alignment and tolerances of mating gaskets and flanges to insure that arcing will not occur at this critical point.

REFERENCES

1. L. Gould, "Handbook on Breakdown of Air in Waveguide Systems," Microwave Associates, 1956.

2. S. C. Brown, "High Frequency Gas Discharge Breakdown" Handbook on Physic vol. XXII, 1955.

3. P. M. Plazman and E. Huber-Solt, "Microwave Breakdown in Non-uniform Electric Fields," Phy. Rev. 119, 1143 (Aug. 1960).

4. M. Gilden, "High Power Capabilities of Waveguide Systems," Quarterly Reports covering period February 1961 to July 1962 NObsr 85190, Microwave Associates.

5. M. Gilden, "High Power Transmission Line and Associated Microwave Parts," Quarterly Reports covering period from July 1961 to September 1962, NObsr 85455, Microwave Associates.

6. W. Beust and W. L. Ford, "Arcing in CW Transmitters," Microwave Journal 4, 91 (Oct. 1961)

7. L. Gould and L. W. Roberts, "Breakdown of Air at Microwave Frequencies," JAP 27, 1162 (Oct. 1956).

8. W. H. Giedt, Principles of Engineering Heat Transfer, D. Van Nostrand Company, New York 1957.

9. G. Southworth, Principles and Applications of Waveguide Transmission pp 362-363, D. Van Nostrand Company, Inc. 1950.

10. P. Marie, "Transition Creant le Mode TE_{01} Circulaire a Partir du Mode TE_{10} Rectanglaire" Onde Electrique Paris, 1957,2,471.

11. S. Rosenbaum, "Theory and Design of Tightly Coupled TE_{10} Rectangular to TE_{01} Circular Mode Transducer" PIBMRI-1022-62 (DA-36-039-SC-85321), Polytechnic Institute of Brooklyn, June 1962.

12. R. M. Collins, "Practical Aspects of High Power Circular Waveguide Systems" NEREM Conference Digest 1962.

13. N. Lipetz, "Progress in Microwave Components" NEREM Conference Digest, 1962.

14. D. A. Lanciani, "Basic Design Criteria for Circular Waveguide Components" Final Report (DA-36-039-SC-5518), Microwave Associates, January 1954.

FIGURE 1

BREAKDOWN OF AIR IN TM010 CAVITY

.025 HEMISPHERE ON FLOOR

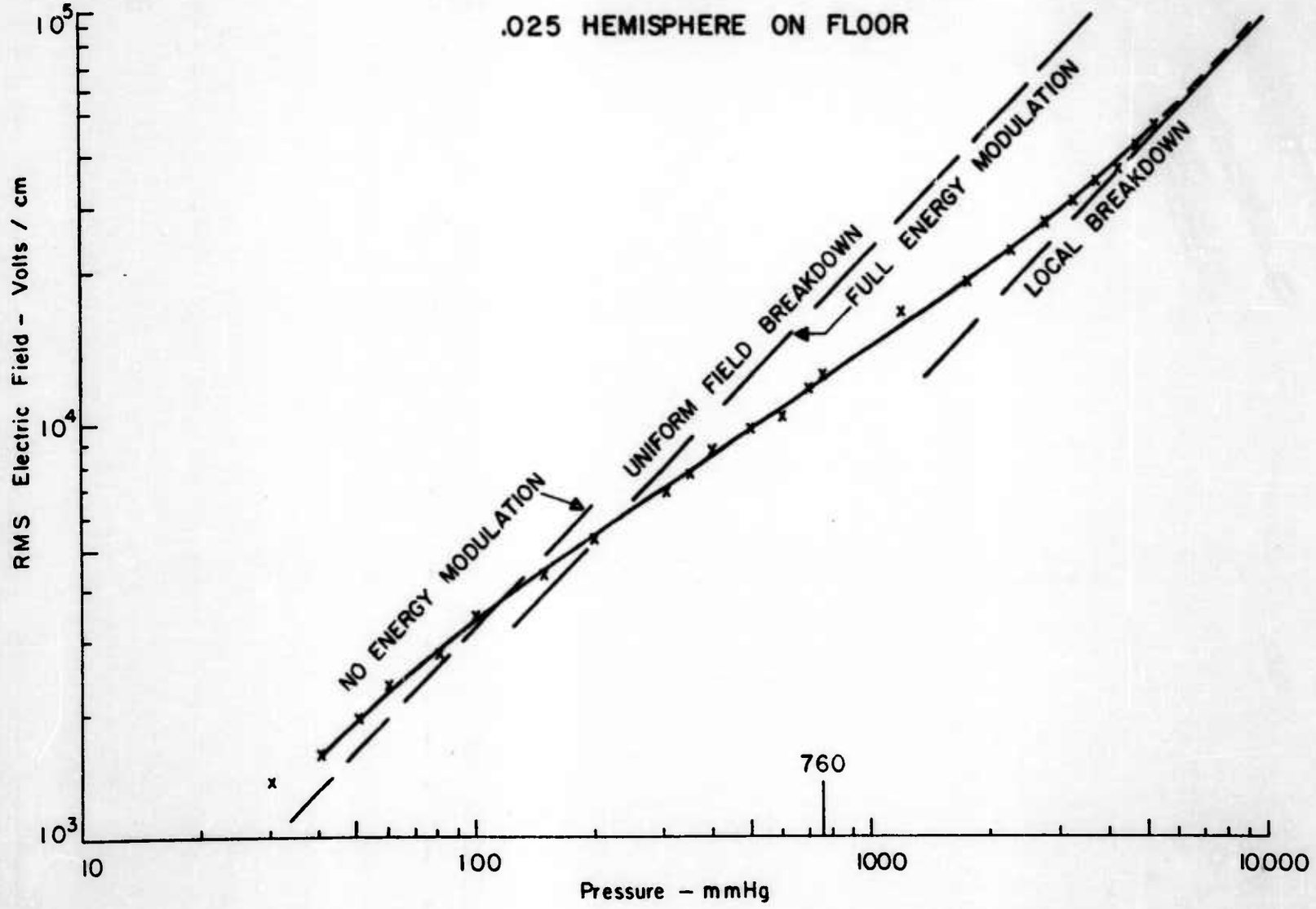

D-18

FIGURE 2

TEMPERATURE OF FOREIGN PARTICLE IN A WAVEGUIDE

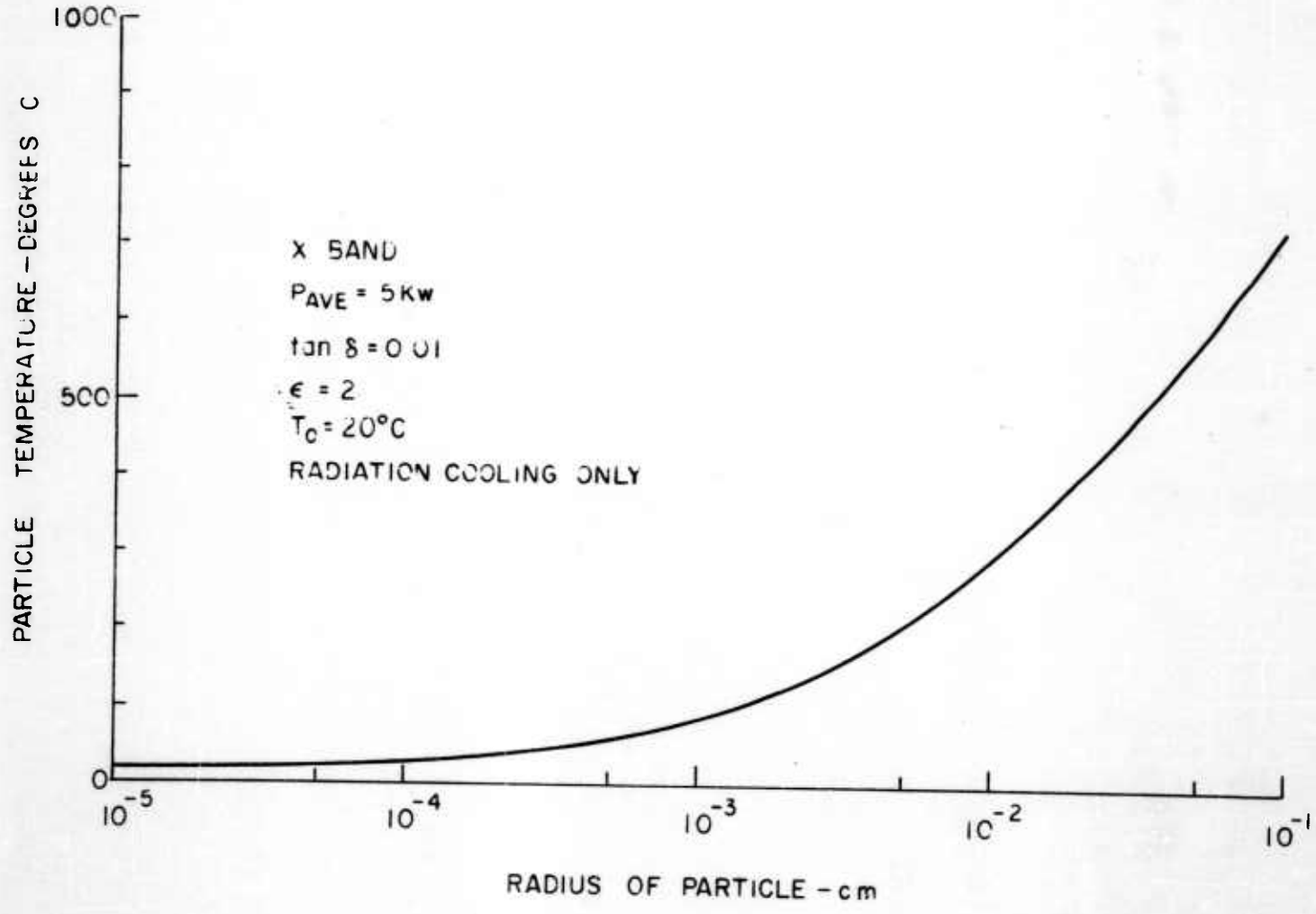

FIGURE 3

VELOCITY OF A TRAVELING ARC
FOR SEVERAL DIFFERENT GASES

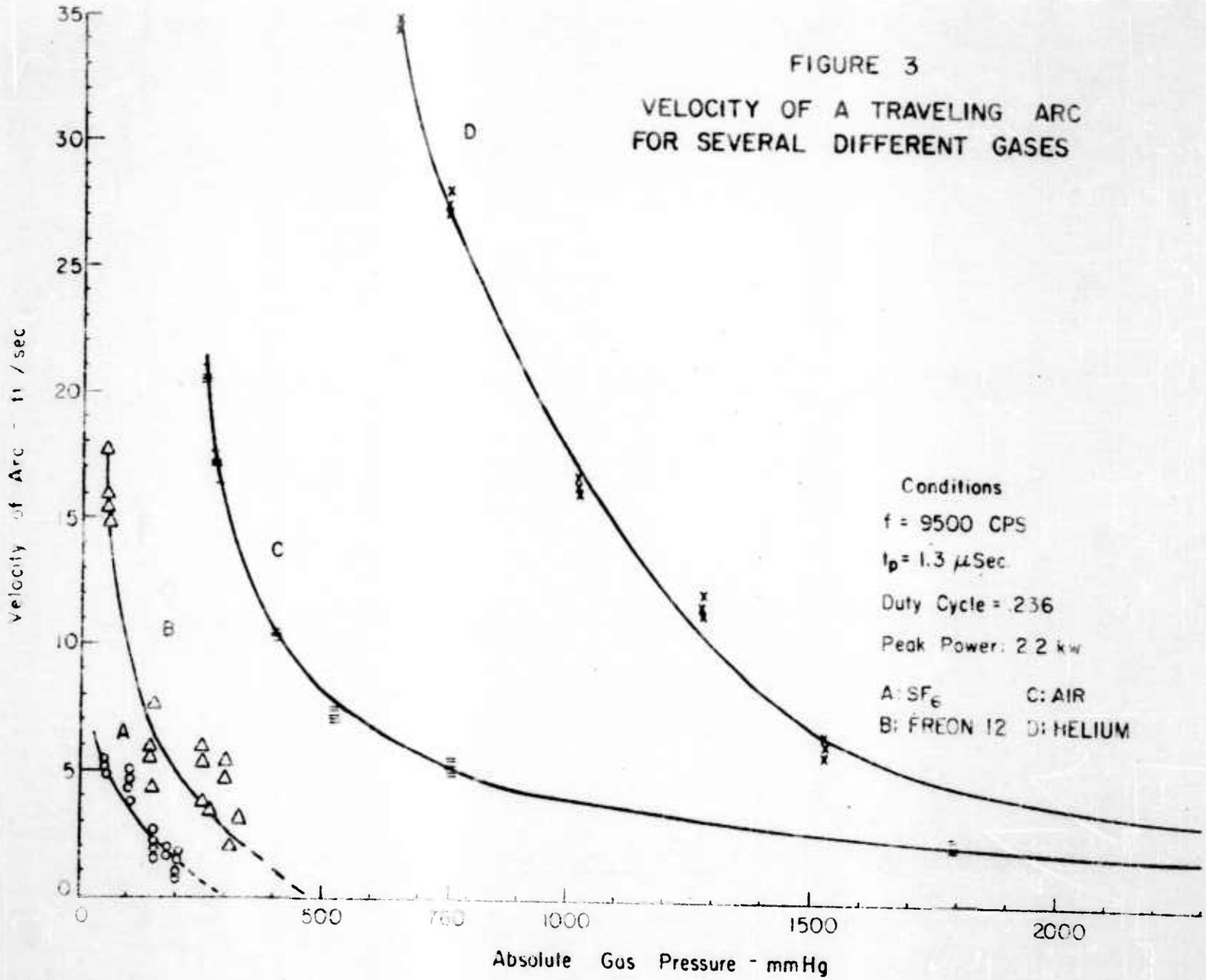

FIGURE 4
ARC VELOCITY IN THE
PRESENCE OF GAS FLOW

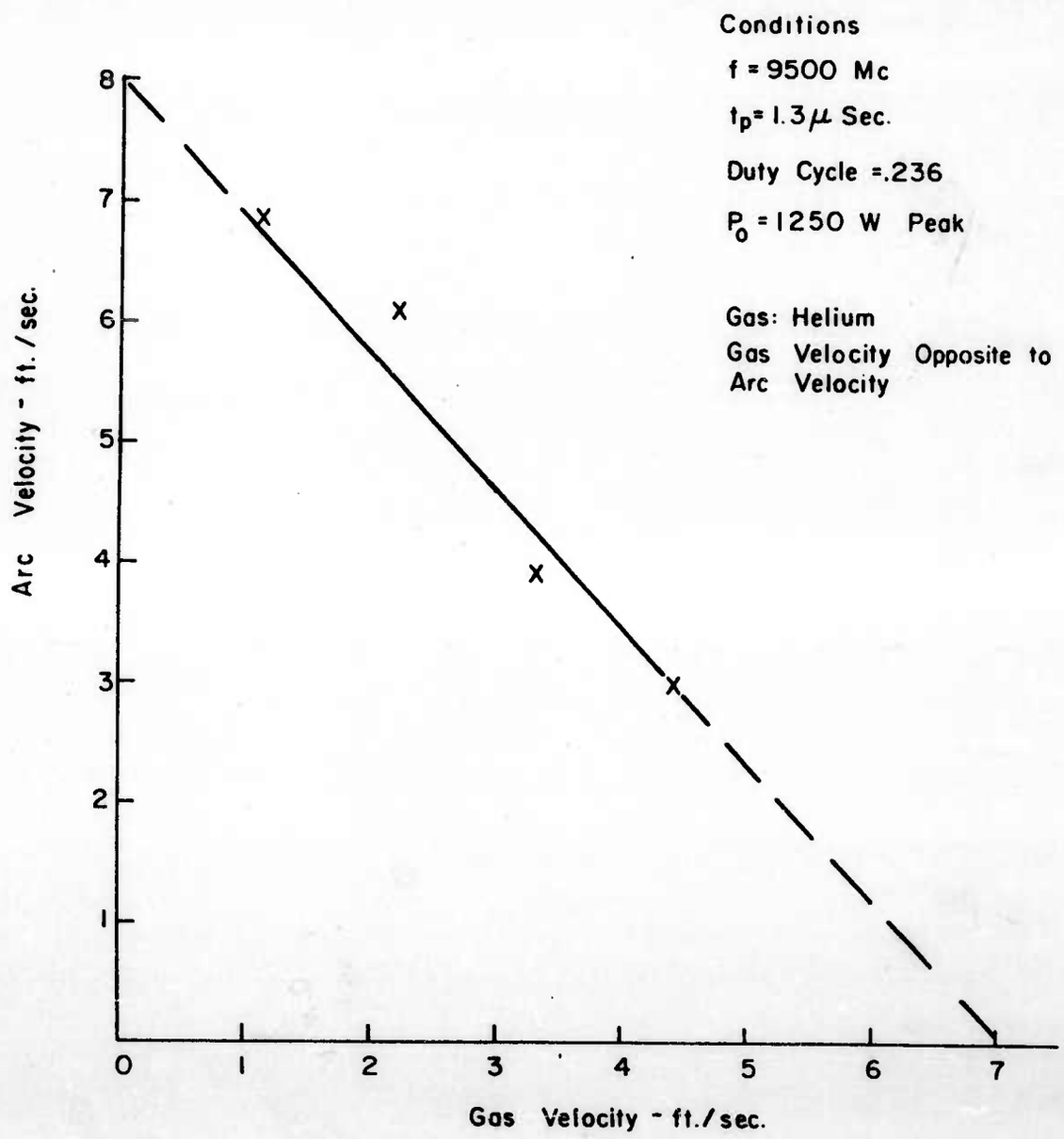

FIGURE 5

POWER DISSIPATION BY INTERNAL FLOW OF GAS, X-BAND

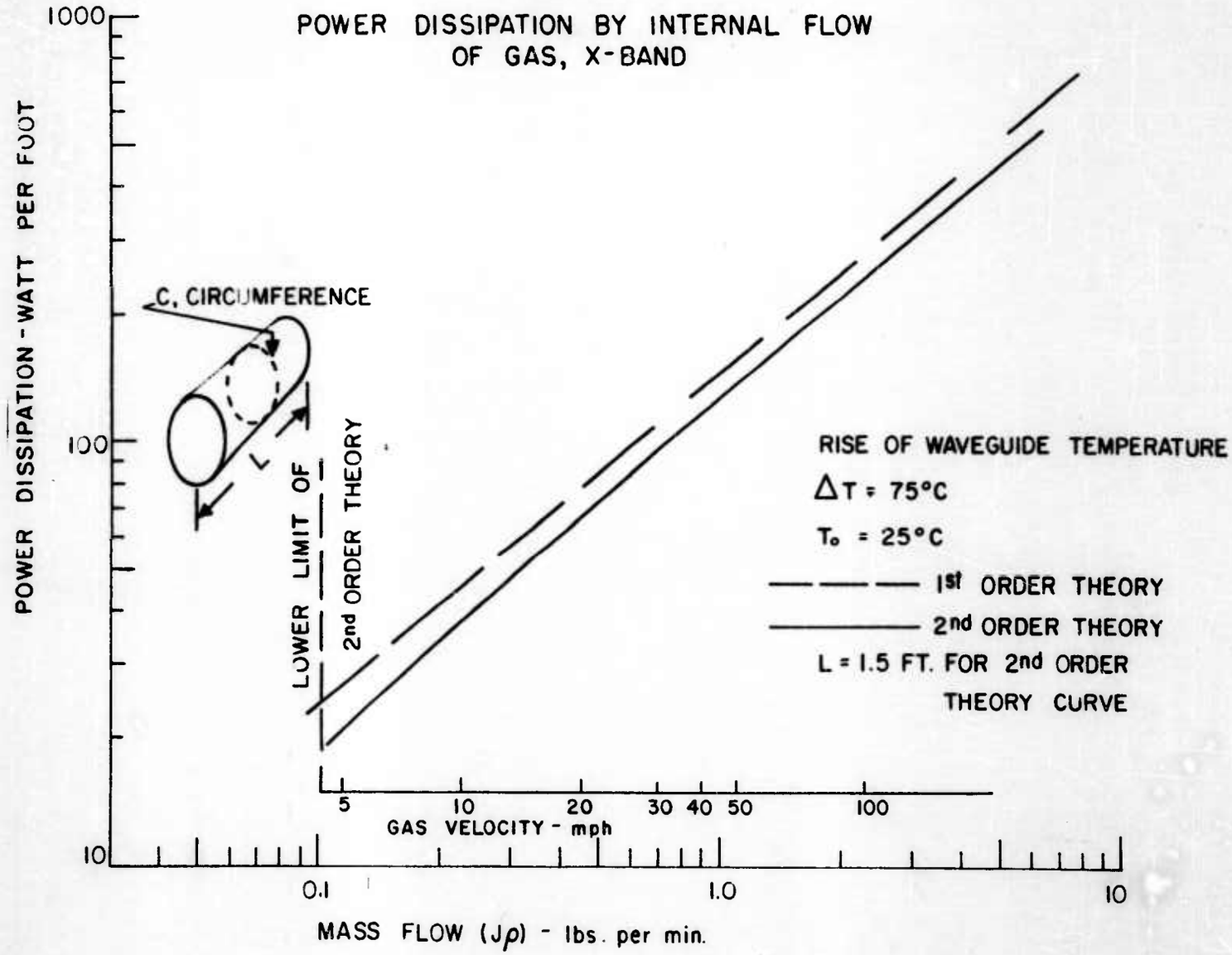

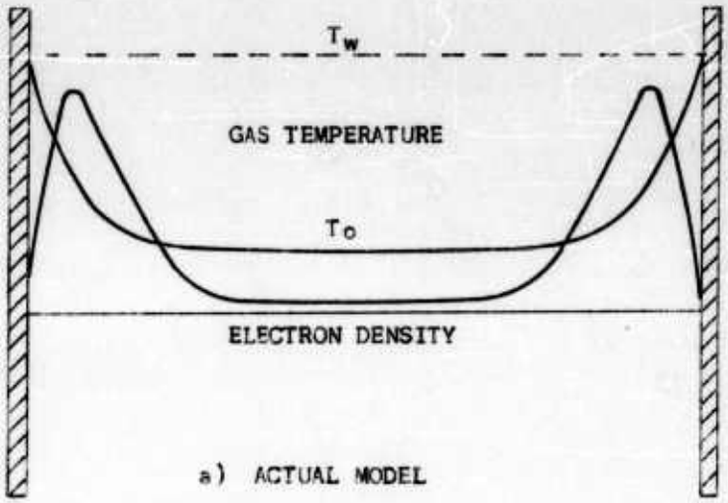

a) ACTUAL MODEL

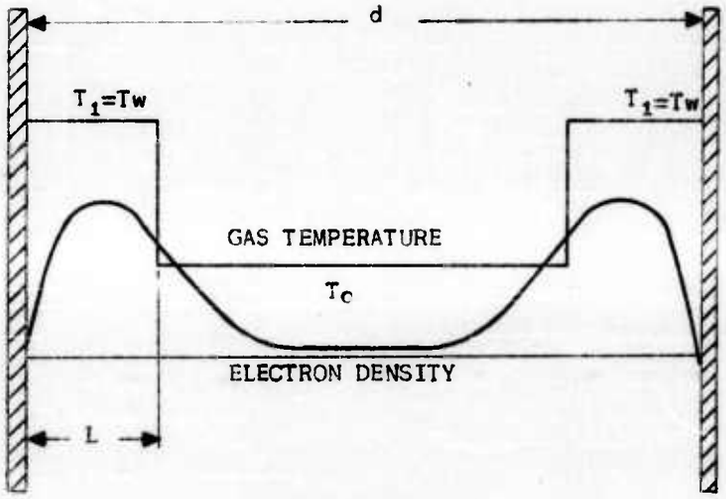

b) APPROXIMATE MODEL

FIGURE 6

PHYSICAL MODELS USED IN ANALYZING
BREAKDOWN AT HOT SURFACES

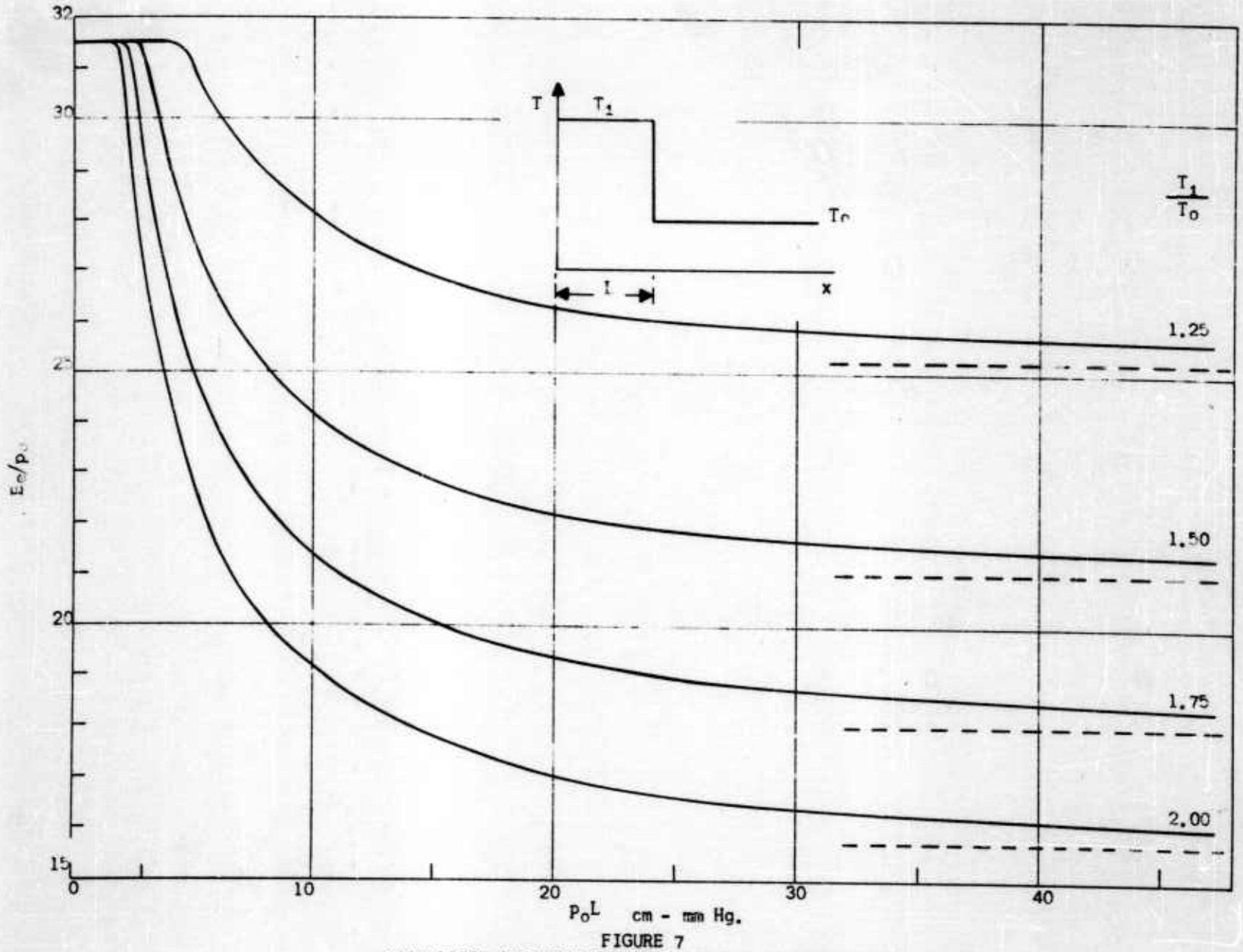

FIGURE 7
NORMALIZED SOLUTION FOR BREAKDOWN AT A HOT SURFACE
(APPROXIMATION BY PIECEWISE LINEAR SOLUTIONS)

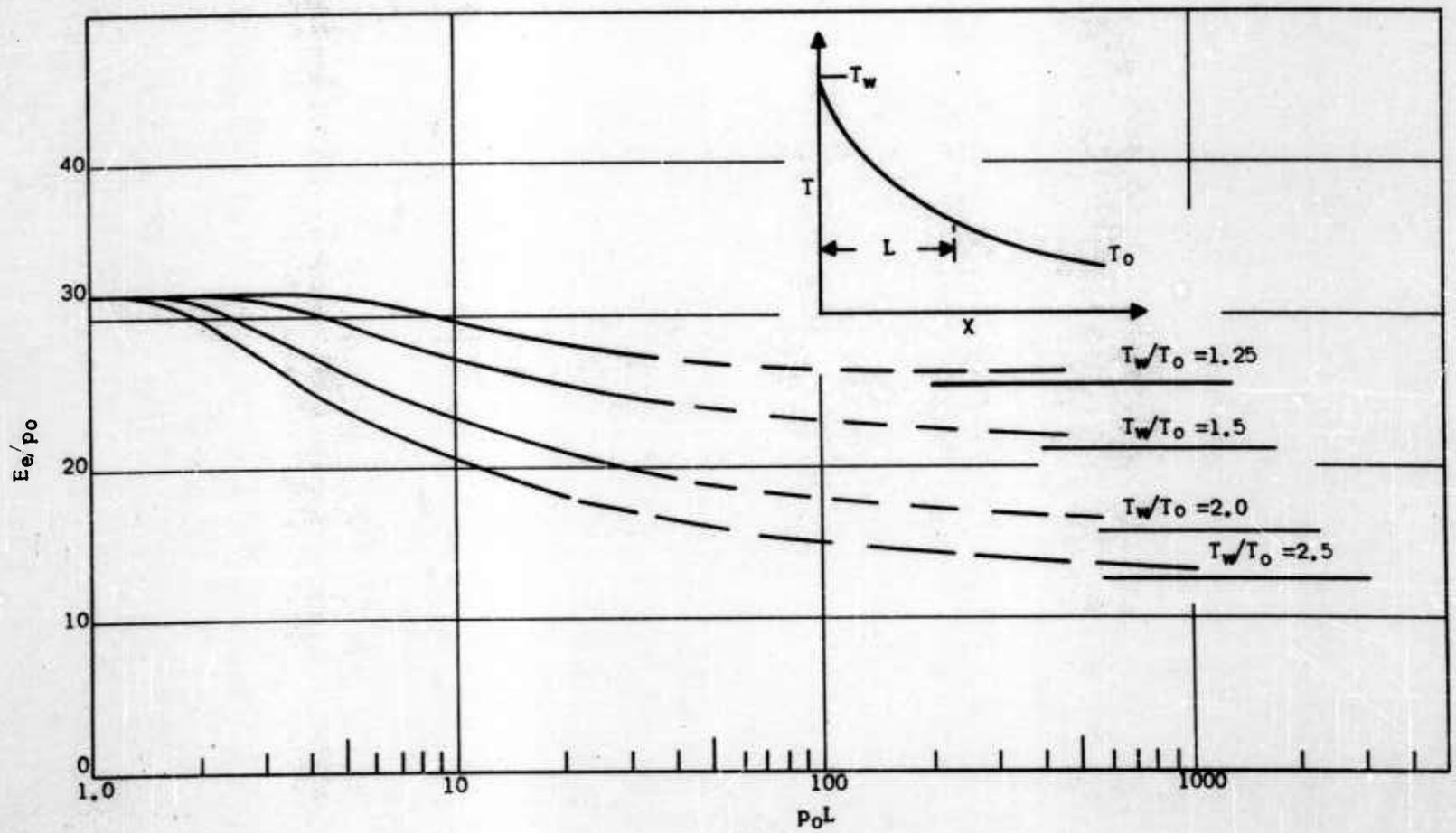

FIGURE 8

NORMALIZED SOLUTION FOR BREAKDOWN AT A HOT SURFACE
(EXACT DIGITAL COMPUTER SOLUTION)

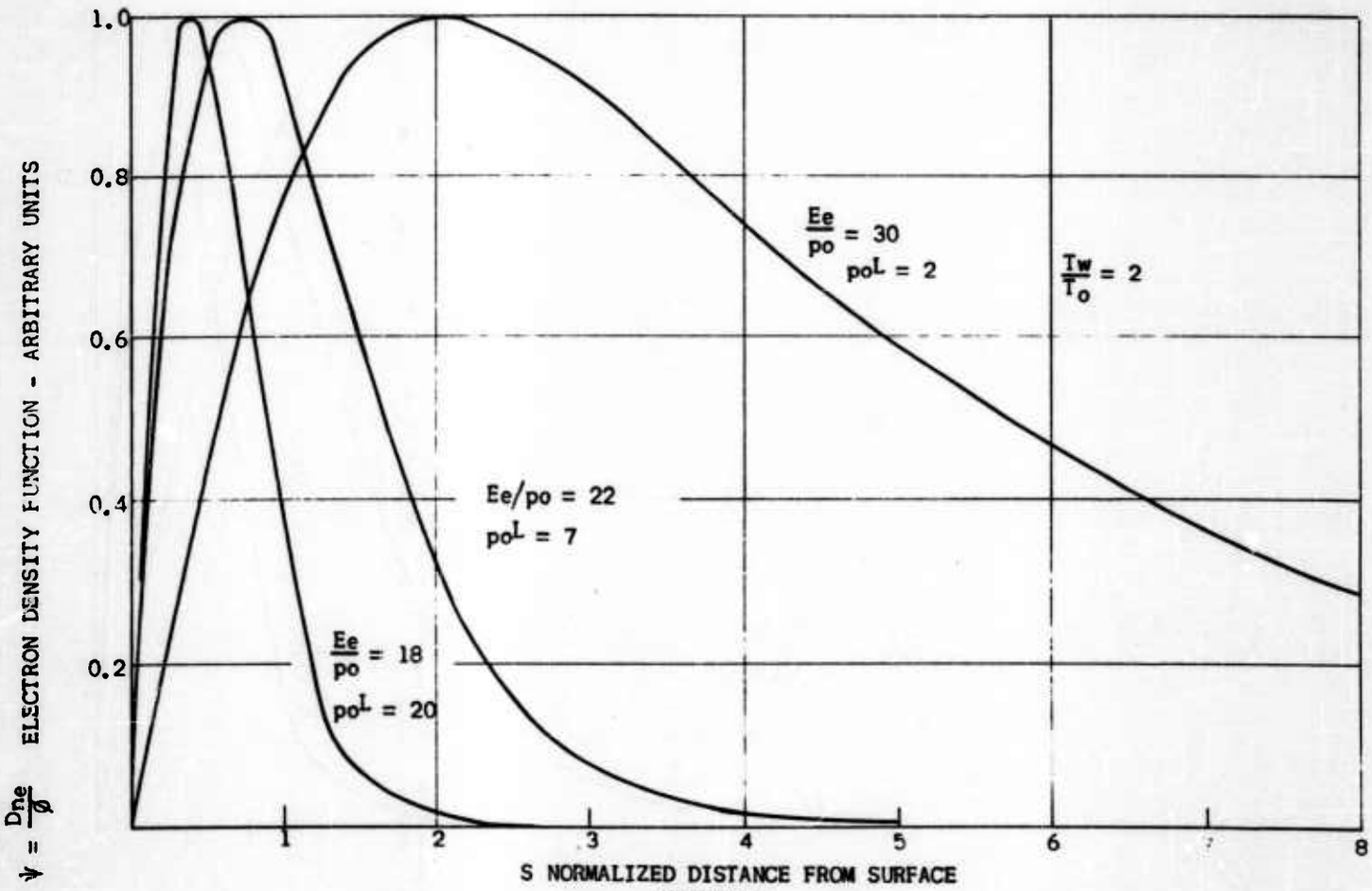

FIGURE 9
VARIATION OF ψ, THE ELECTRON DENSITY FUNCTION NEAR THE HOT SURFACE

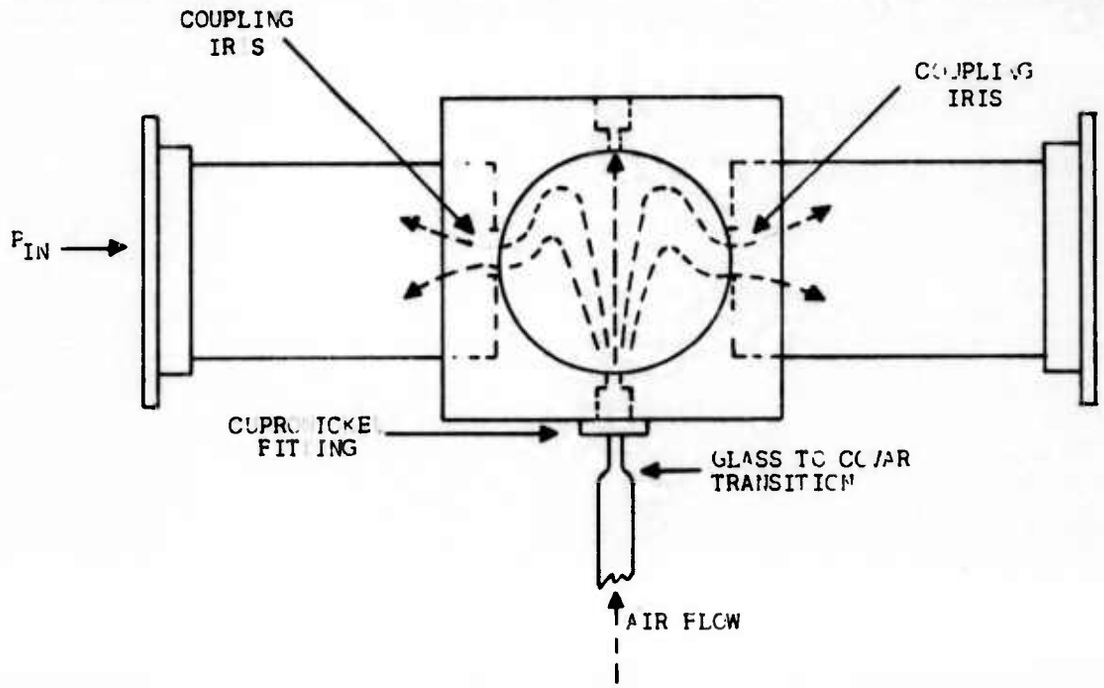

C BAND TM_{010} RESONANT CAVITY COVER REMOVED

RESONANT FREQUENCY:	5.5 G
CAVITY DIAMETER	1.643
CAVITY HEIGHT:	.300"
MATERIAL:	BRASS

FIGURE 0

RESONANT CAVITY WITH AIR FLOW USED FOR HOT SURFACE BREAKDOWN STUDY

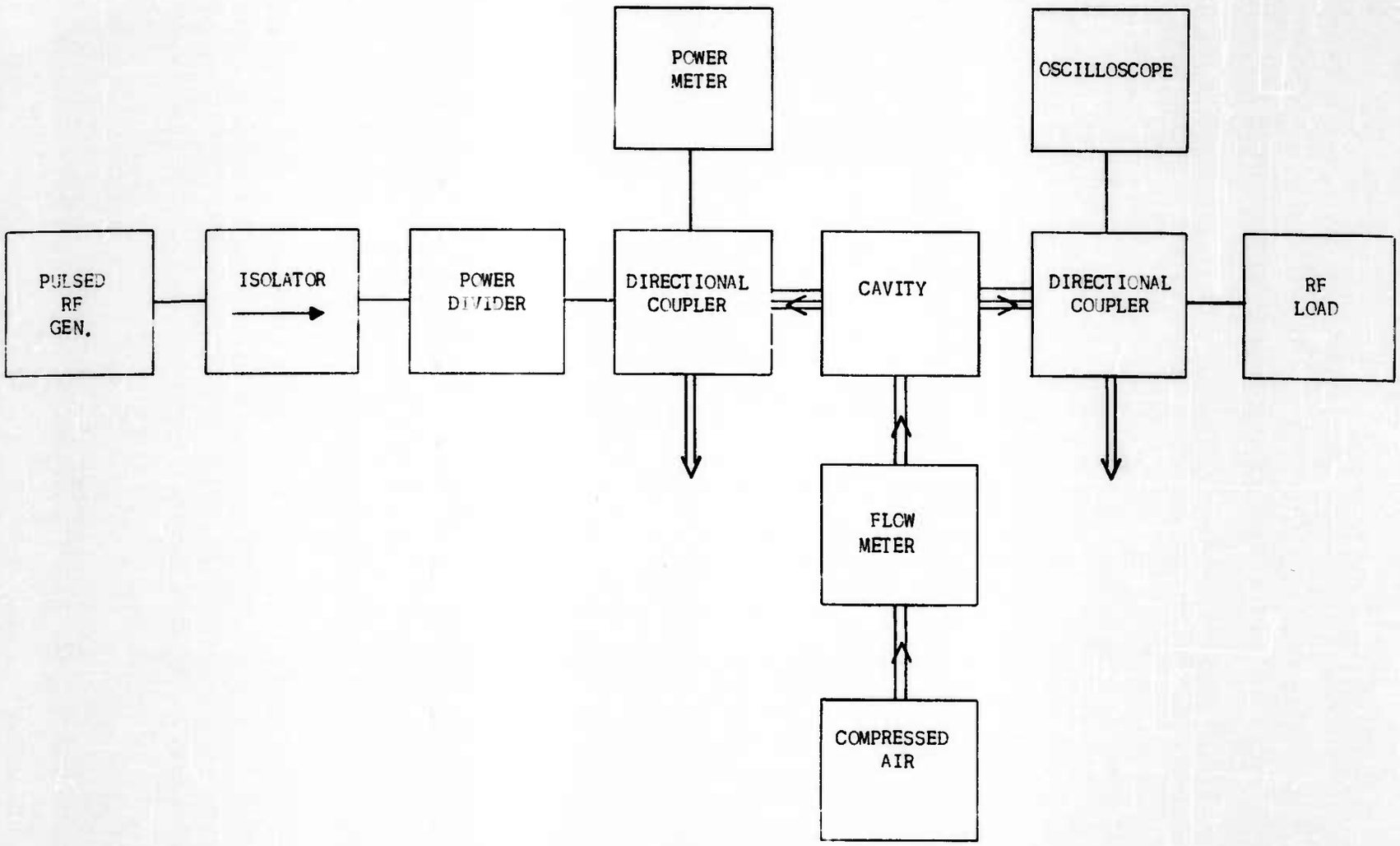

FIGURE 11

MICROWAVE CIRCUIT USED FOR BREAKDOWN STUDY

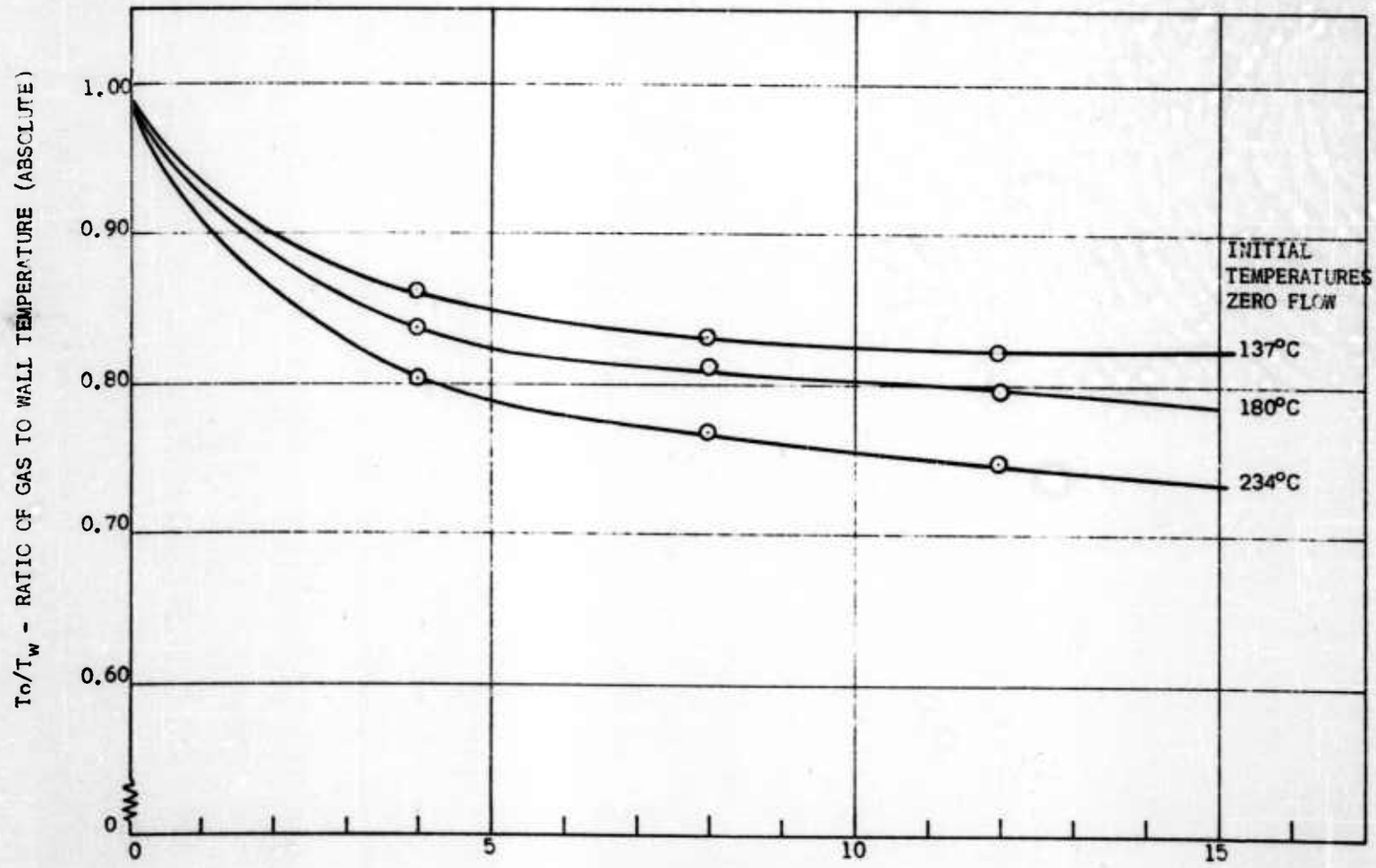

FIGURE 12 CALIBRATION OF CAVITY AND GAS STREAM TEMPERATURE

FIGURE 13

NORMALIZED RESULTS OF BREAKDOWN AT A HOT SURFACE
IN THE PRESENCE OF GAS FLOW (T_{wo}= 182°C)

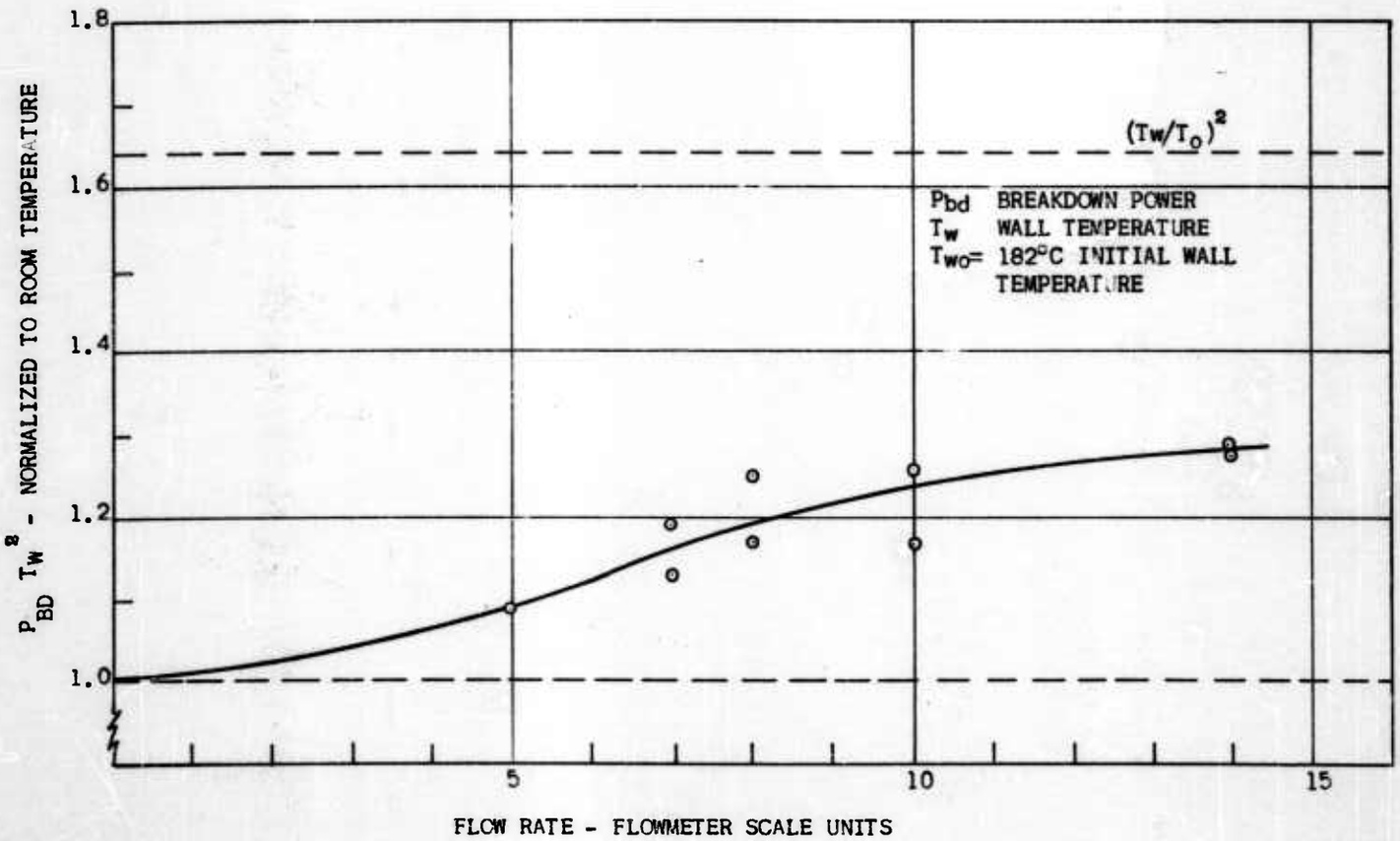

FIGURE 14

NORMALIZED RESULTS OF BREAKDOWN AT A HOT SURFACE
IN THE PRESENCE OF GAS FLOW (T_{wo}= 220°C)

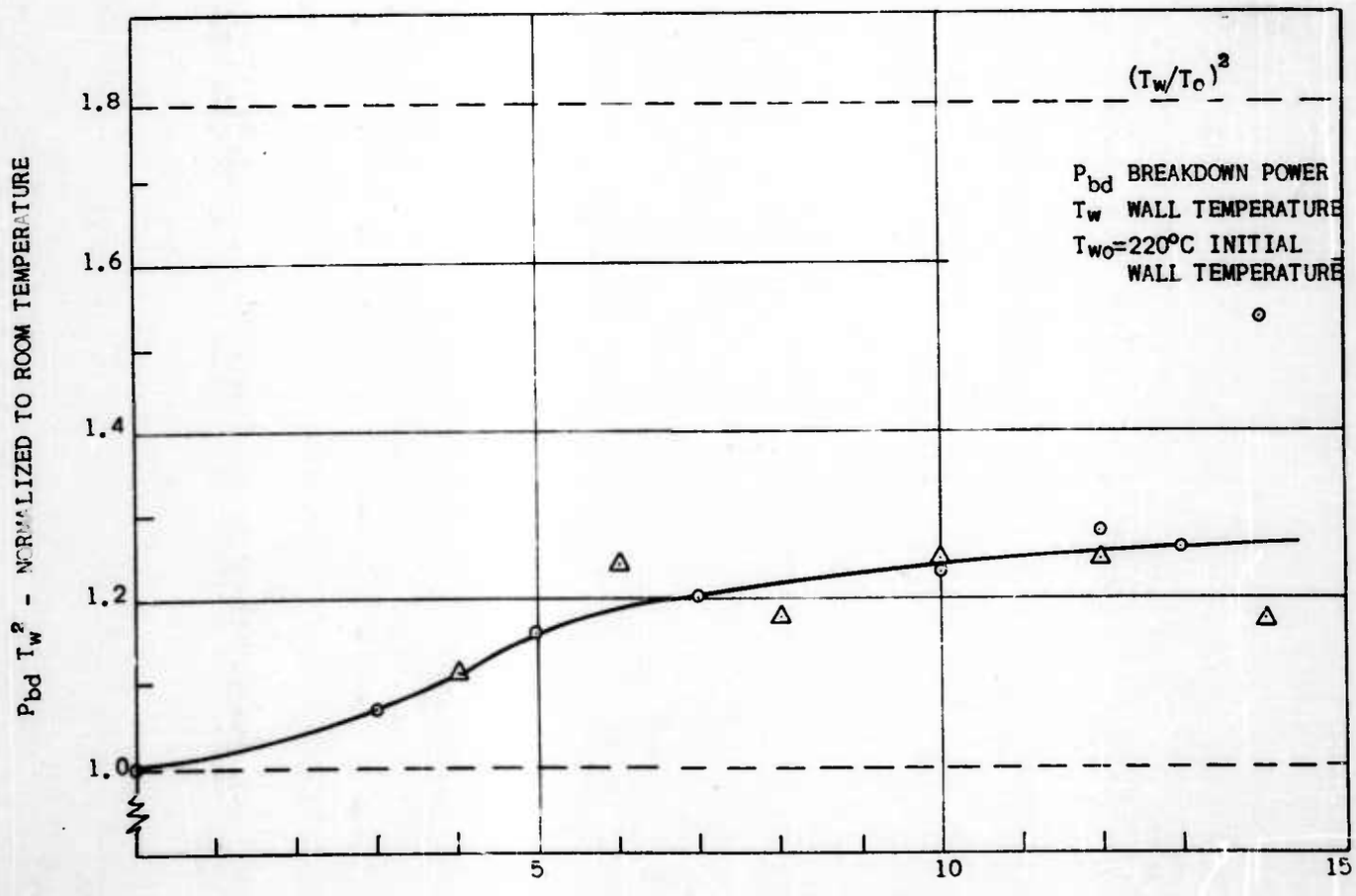

FIGURE 15

NORMALIZED RESULTS OF BREAKDOWN AT A HOT SURFACE
WITH ZERO GAS FLOW

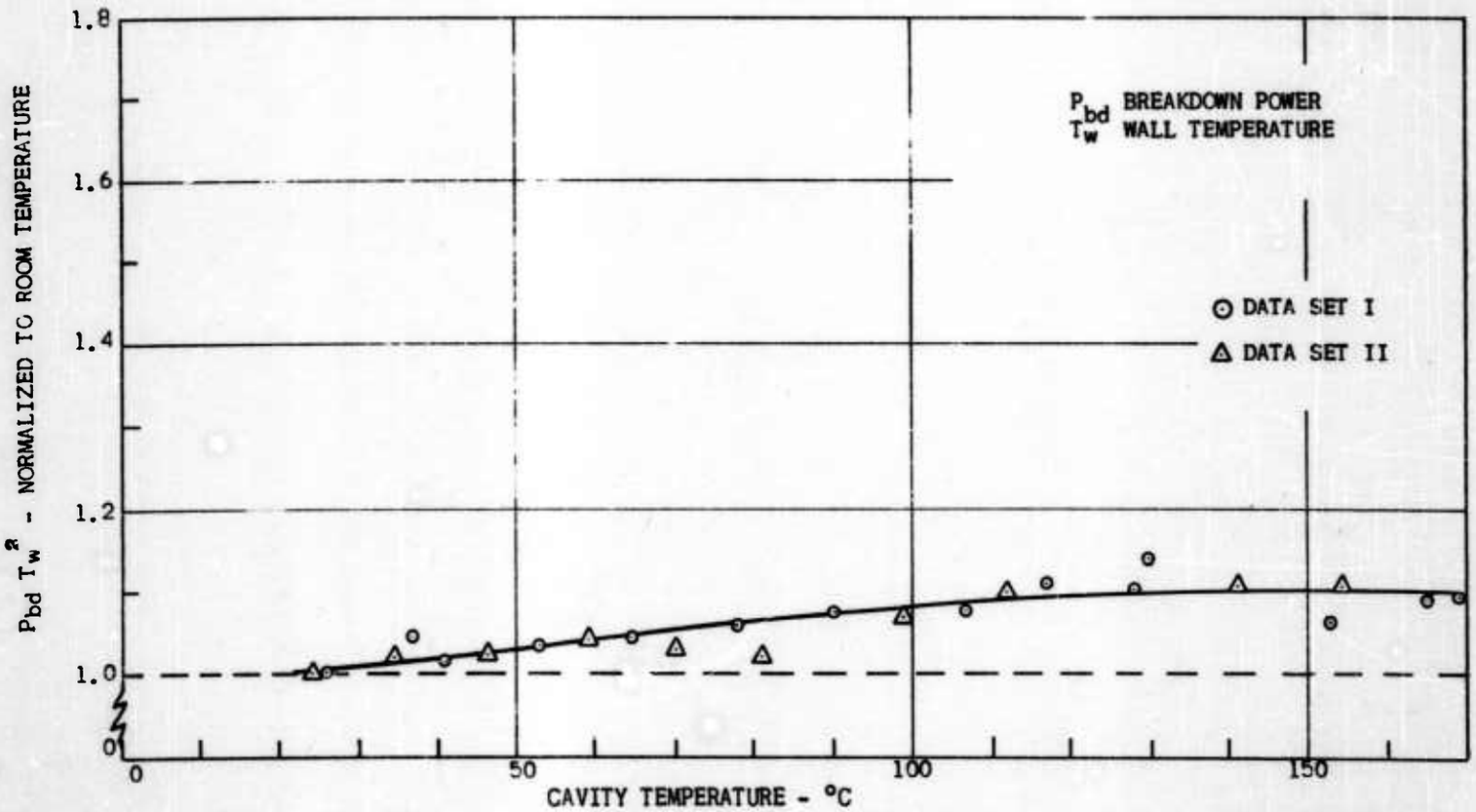

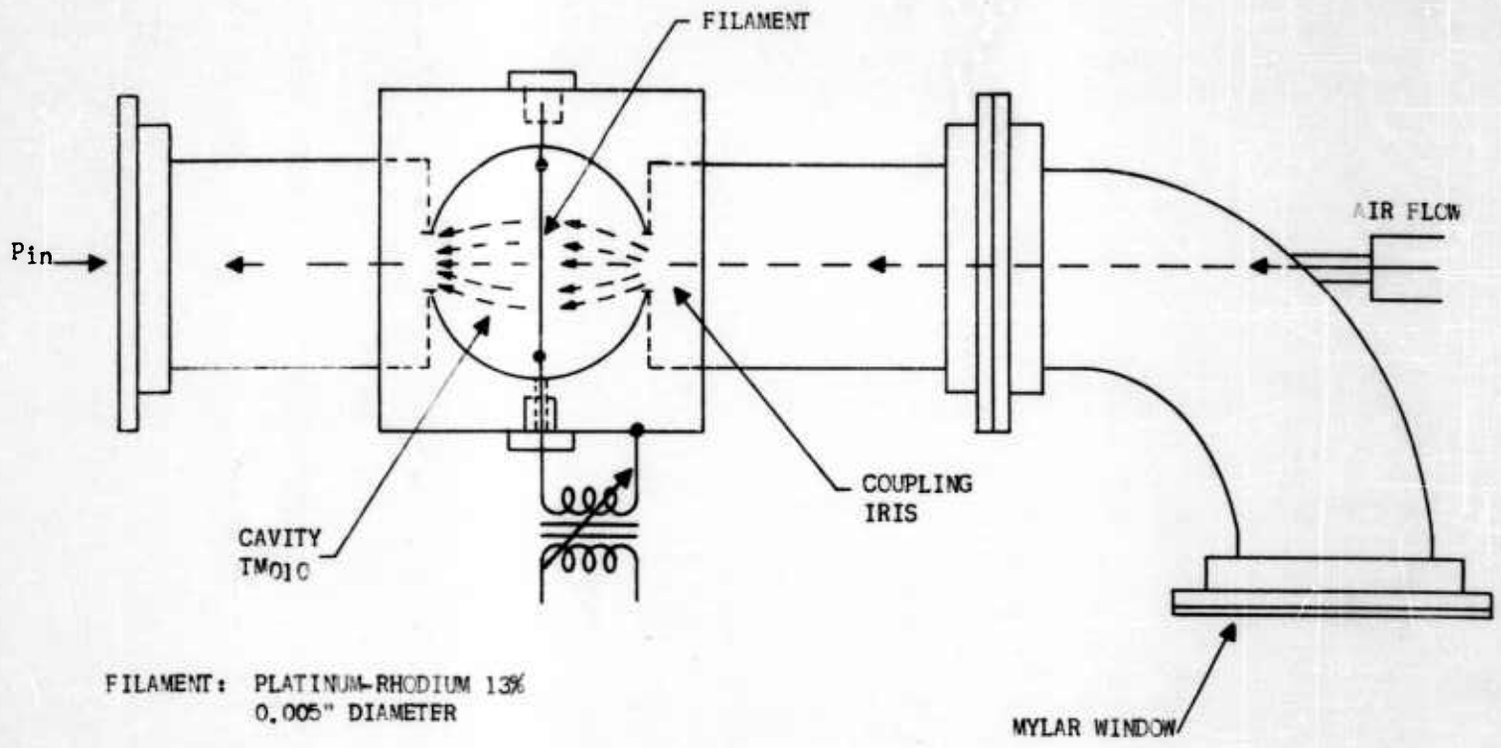

FIGURE 16

RESONANT CAVITY WITH HOT WIRE FOR STUDYING BREAKDOWN
IN THE PRESENCE OF AIR FLOW

FIGURE 17

RESULTS OF BREAKDOWN MEASUREMENTS
WITH A HOT WIRE IN THE PRESENCE OF GAS FLOW

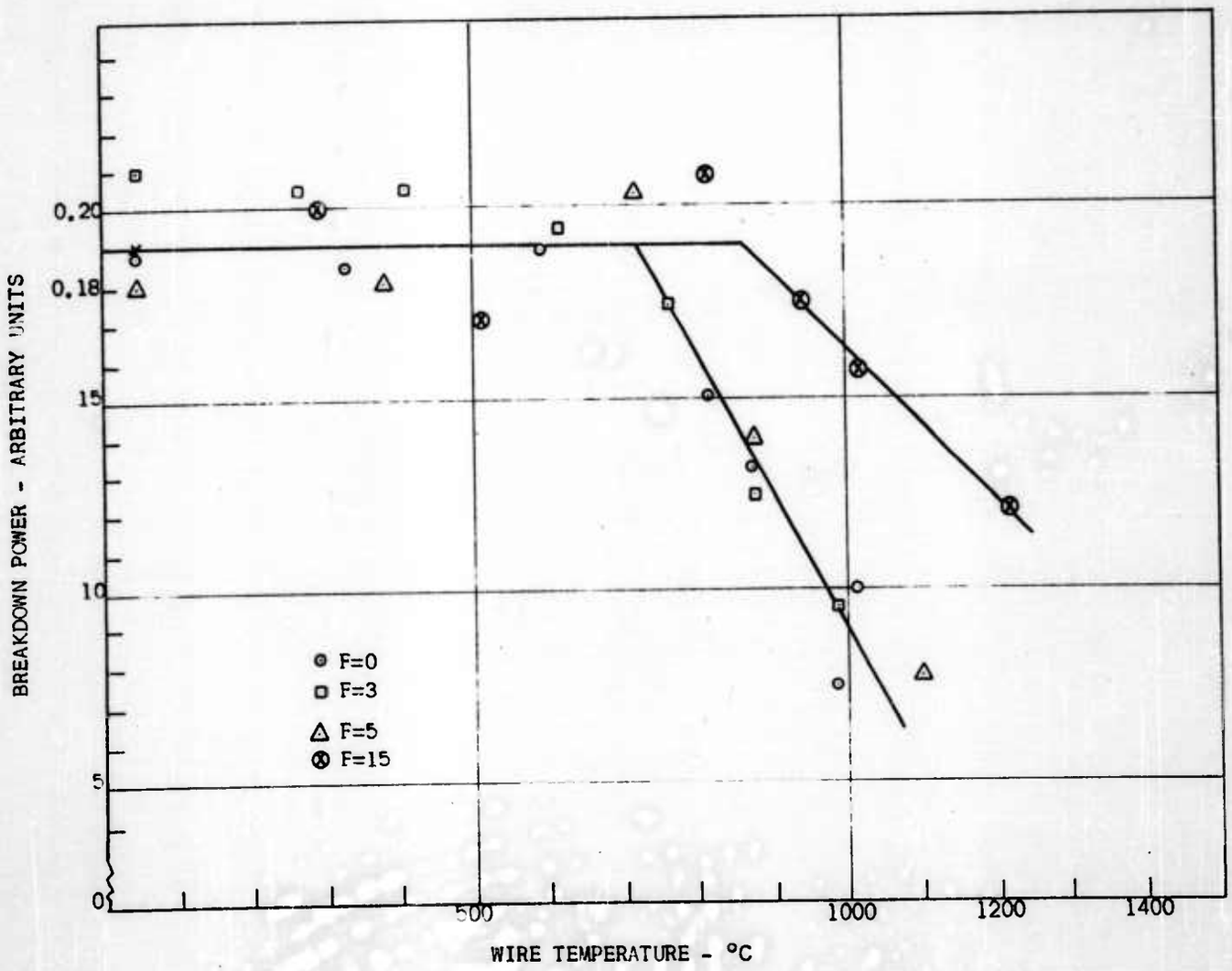

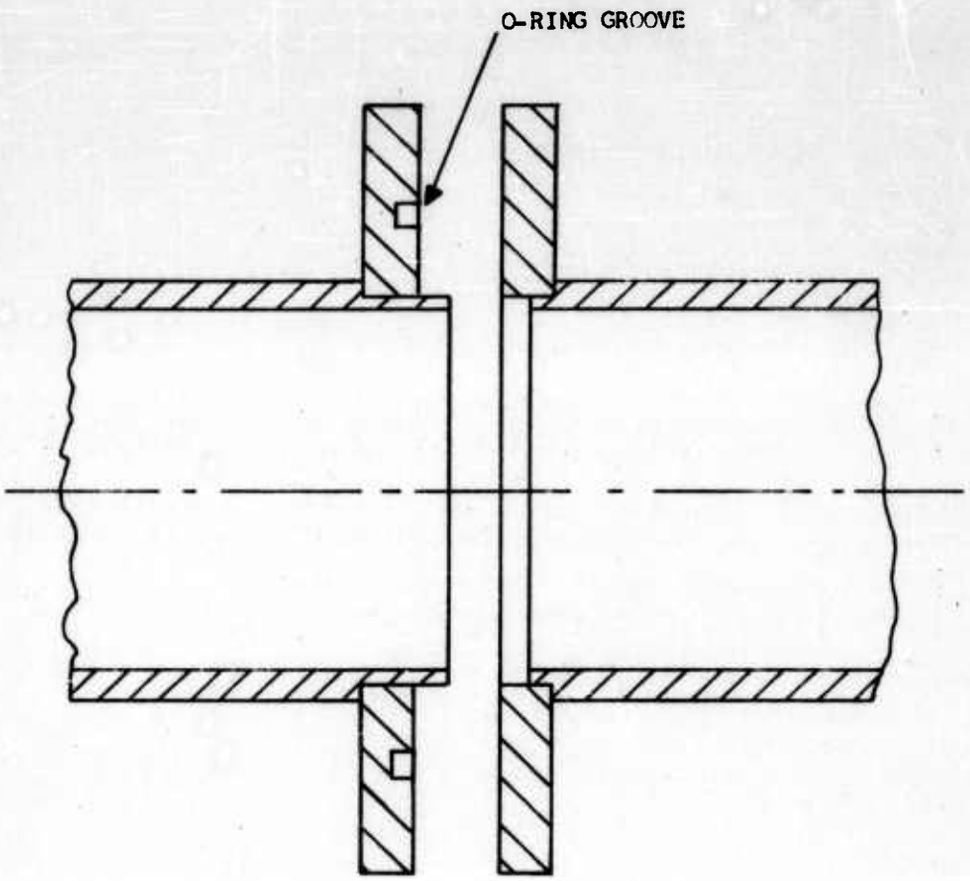

FIGURE 18

$TE_{01}°$ WAVEGUIDE JOINT - MALE AND FEMALE

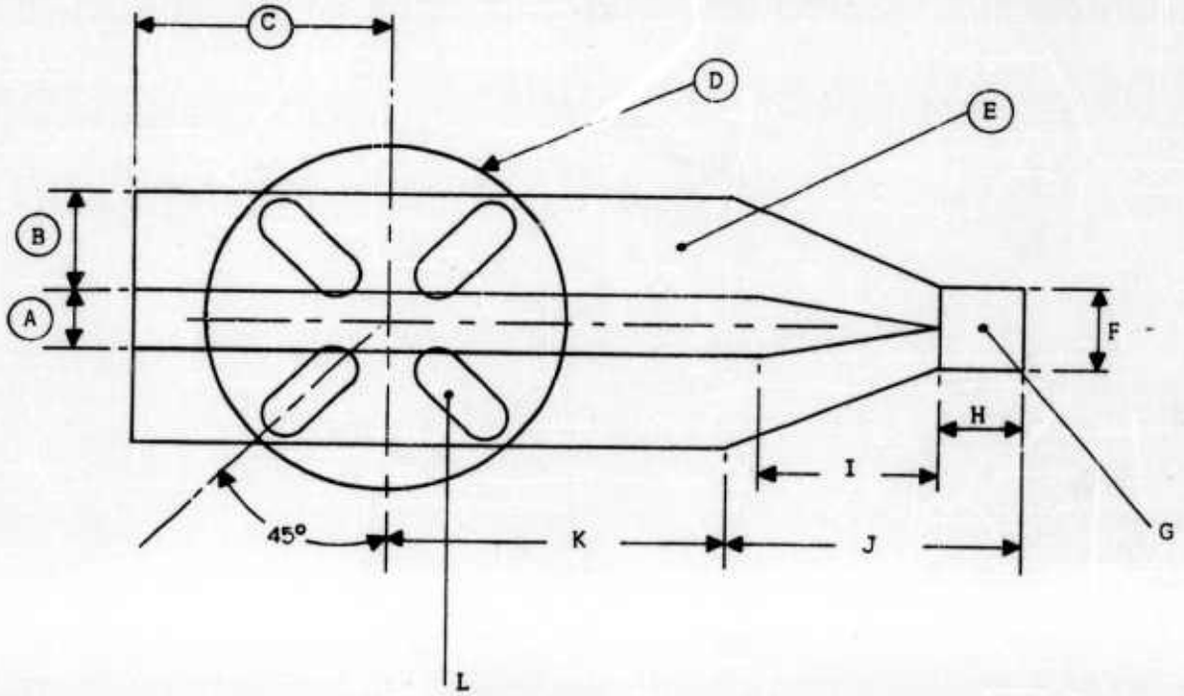

FIGURE 19a

$TE_{10}^{\square}$ - TE_{01}° MODE TRANSDUCER

SKELETON VIEW

FIGURE 19b

$TE^{\square}_{10}$ TE°_{01} MODE TRANSDUCER DIMENSIONS

DIMENSION	SCALED MODEL (8.8 Gc)	FINAL MODEL (7.8 Gc)
A	.212	.242
B	.564	.644
C	1.608	1.802
D	2.410 DIA.	2.680 DIA.
E - CHANNEL DEPTH	1.075	1.228
F	.497	.497
G - DEPTH	1.100	1.173
H	.402	.479
I	.813	1.060
J	2.040	2.350
K	1.222	1.403
L		
PLATE THICKNESS	.077	.085
SLOT HEIGHT	.312	.344
SLOT WIDTH	.756	.840
SLOT LOCATION	1.156 DIA. B.C.	1.320 DIA. B.C.

ALL DIMENSION IN INCHES

FIGURE 20

MODE PURITY AND VSWR FOR $TE_{10}^{\square}$ - TE_{01}° TRANSDUCER (SCALED VERSION)

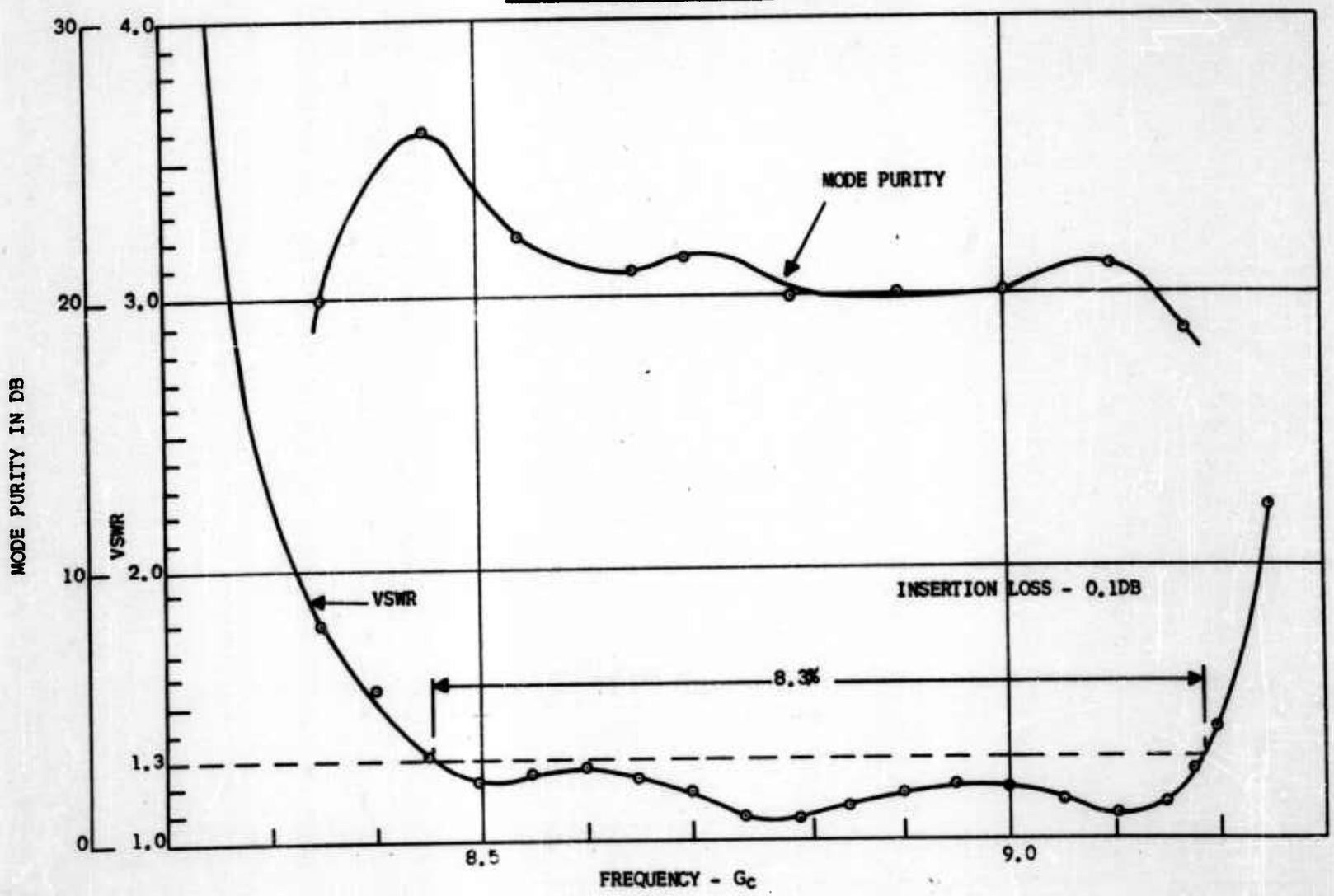

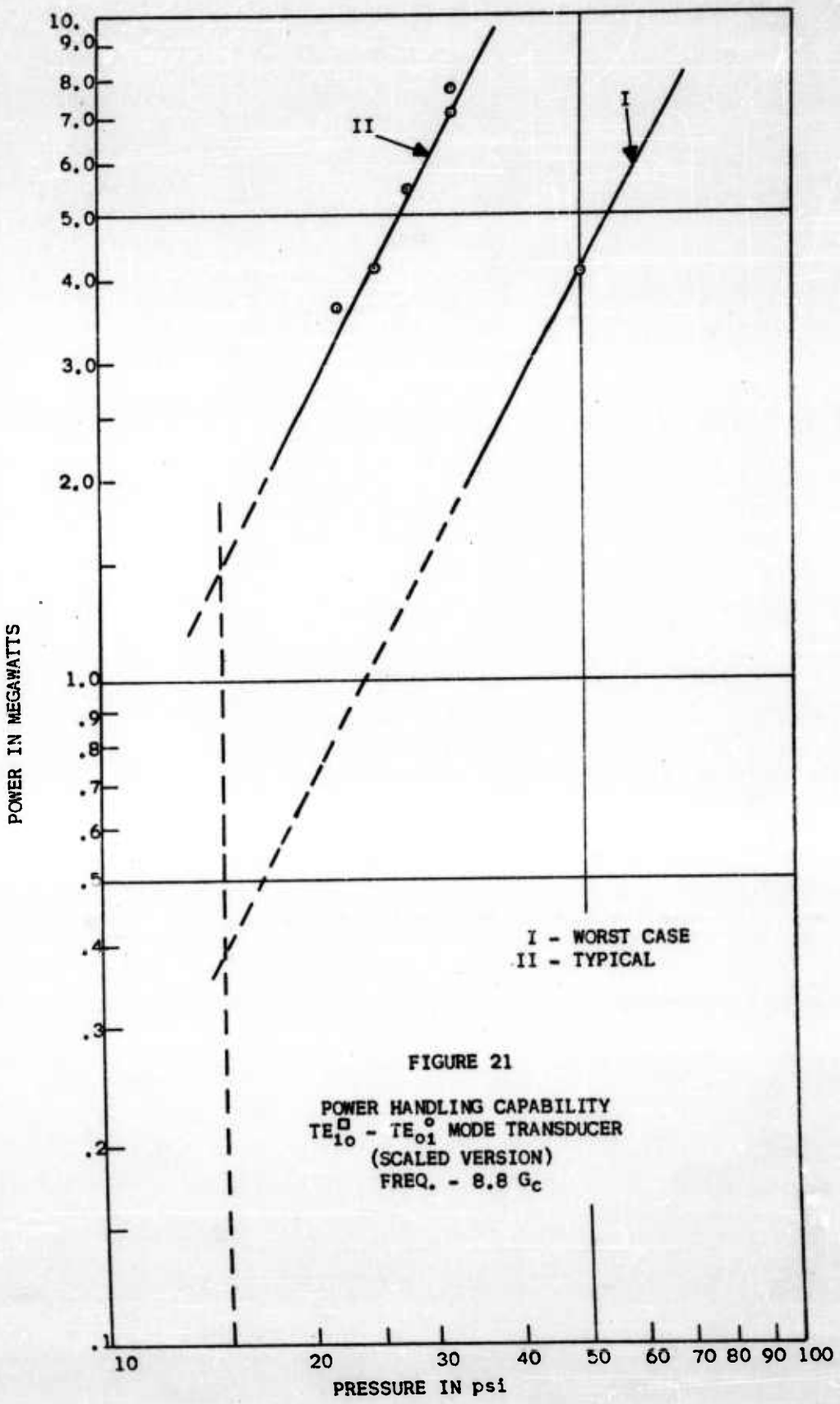

FIGURE 21

POWER HANDLING CAPABILITY
$TE_{10}^{\square}$ - TE_{01}° MODE TRANSDUCER
(SCALED VERSION)
FREQ. - 8.8 G_c

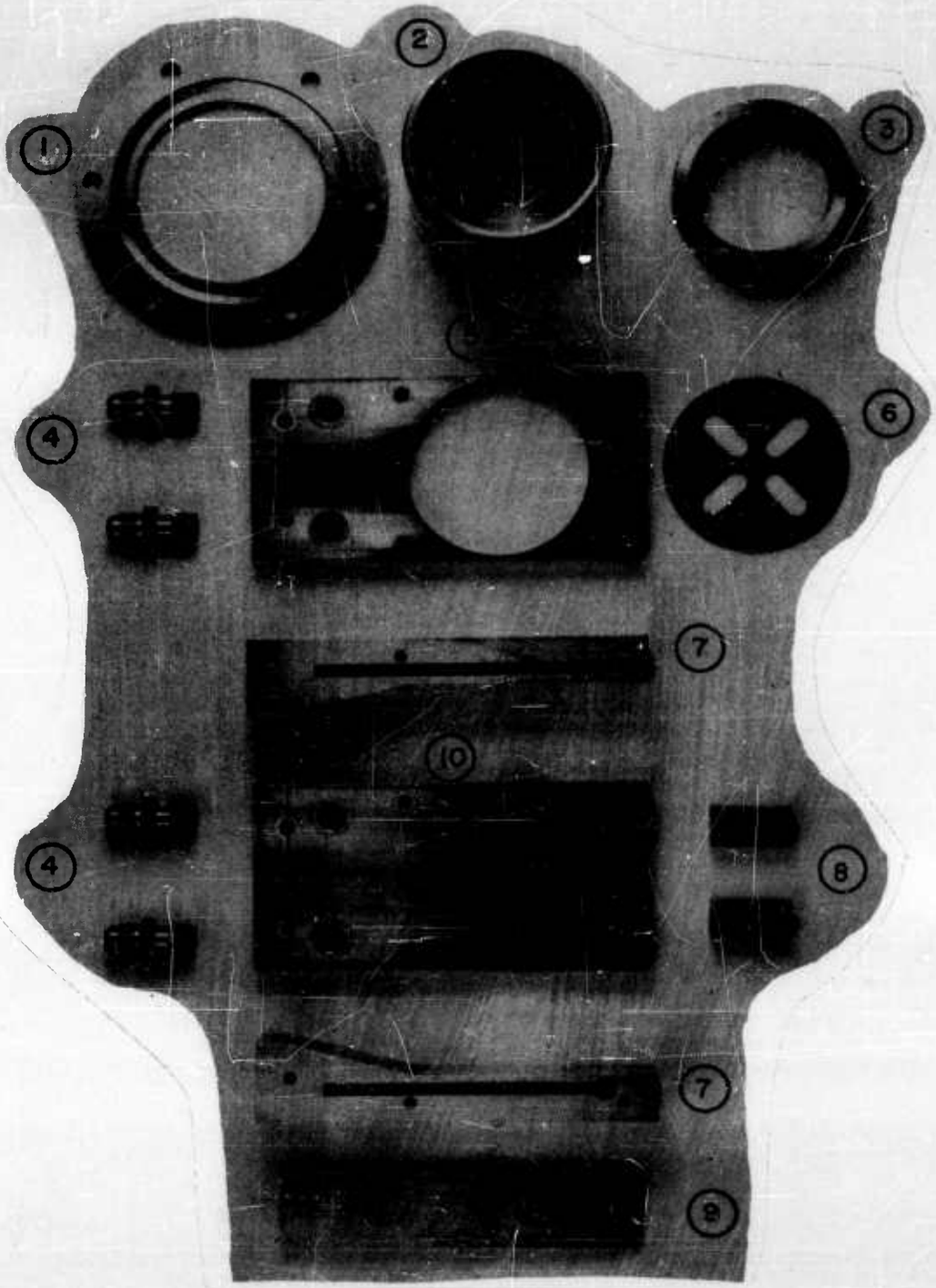

FIGURE 22a

TE_{10} — T_{01}^{o} MODE TRANSDUCER - PARTS

ITEM	DESCRIPTION
1.	Male Output Flange
2.	Output Waveguide
3.	Tuning Ring
4.	3/8" Water Fittings
5.	Top Plate
6.	Coupling Plate
7.	Side Walls
8.	Shorting Slugs
9.	Bifurcation
10.	Bottom Plate

FIGURE 22b

LIST OF PARTS SHOWN IN FIGURE 22a

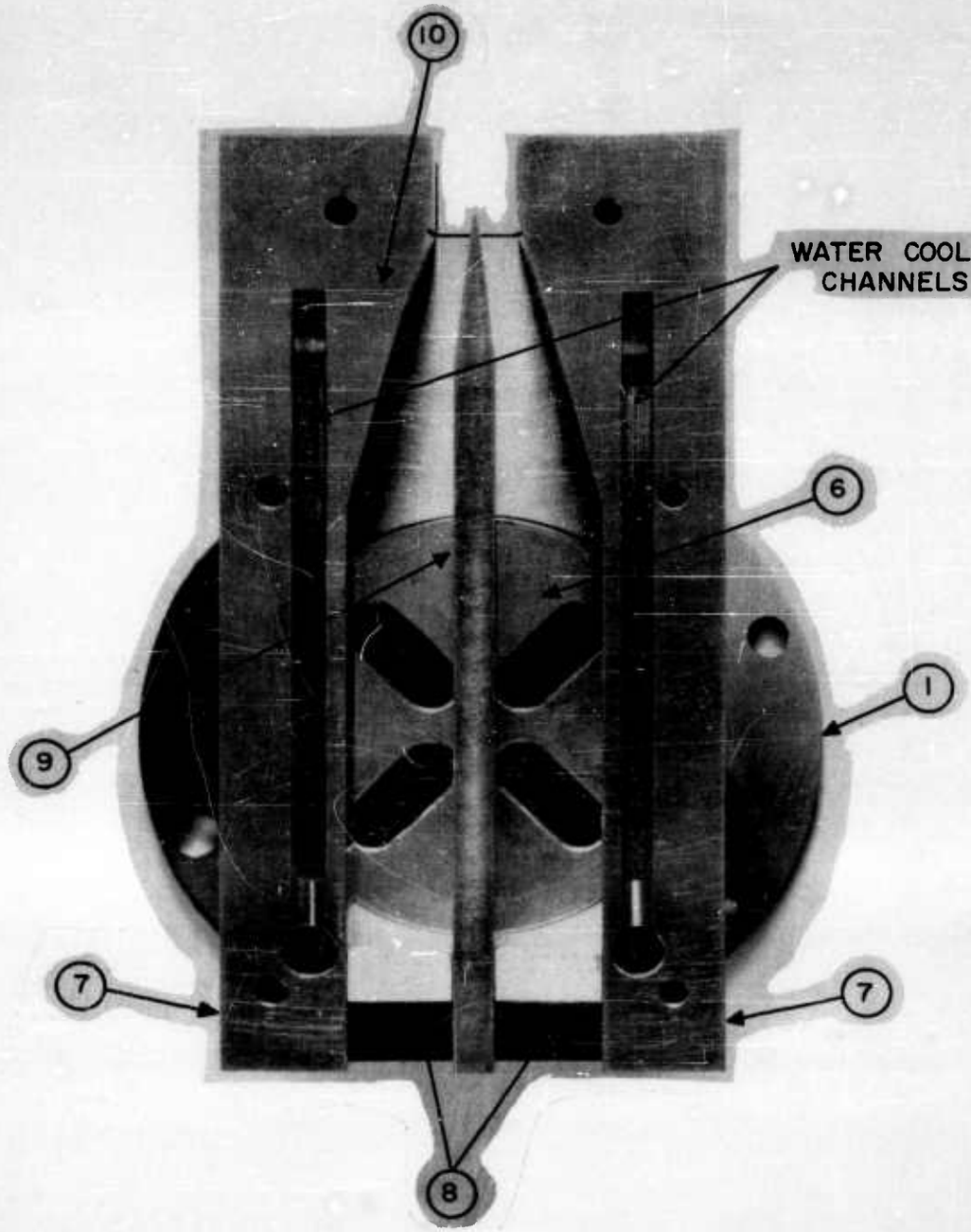

FIGURE 23

$TE_{10}^{\square}$ — TE_{01}° MODE TRANSDUCER- PARTIALLY ASSEMBLED
(BOTTOM VIEW)

FIGURE 24

MODE TRANSDUCER CHARACTERISTICS
AS A FUNCTION OF
ATTENUATION AND COUPLING TO SPURIOUS MODE

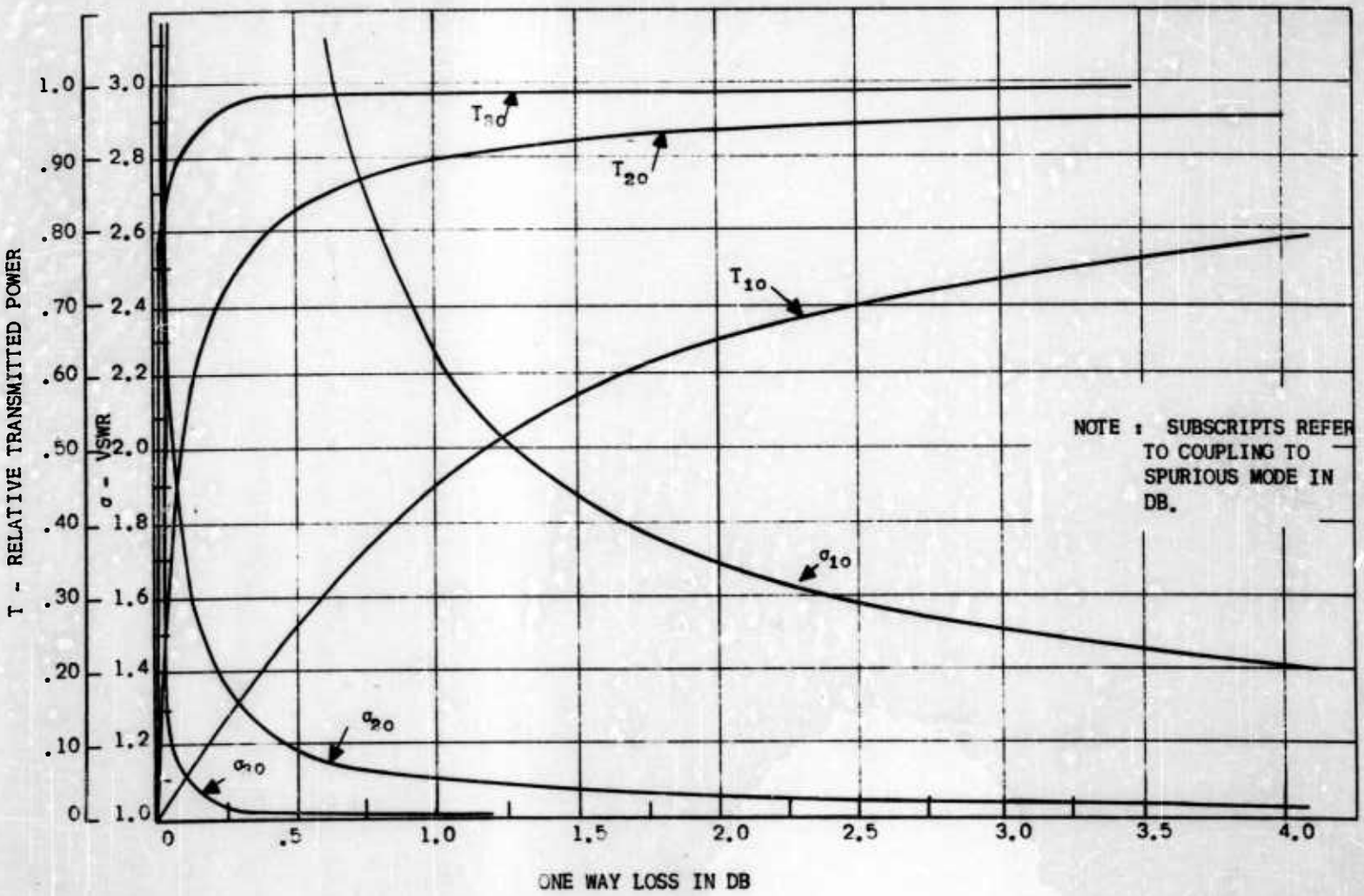

FIGURE 25 POWER GAIN FOR DETERMINING BREAKDOWN THRESHOLD FOR A SPURIOUS MODE

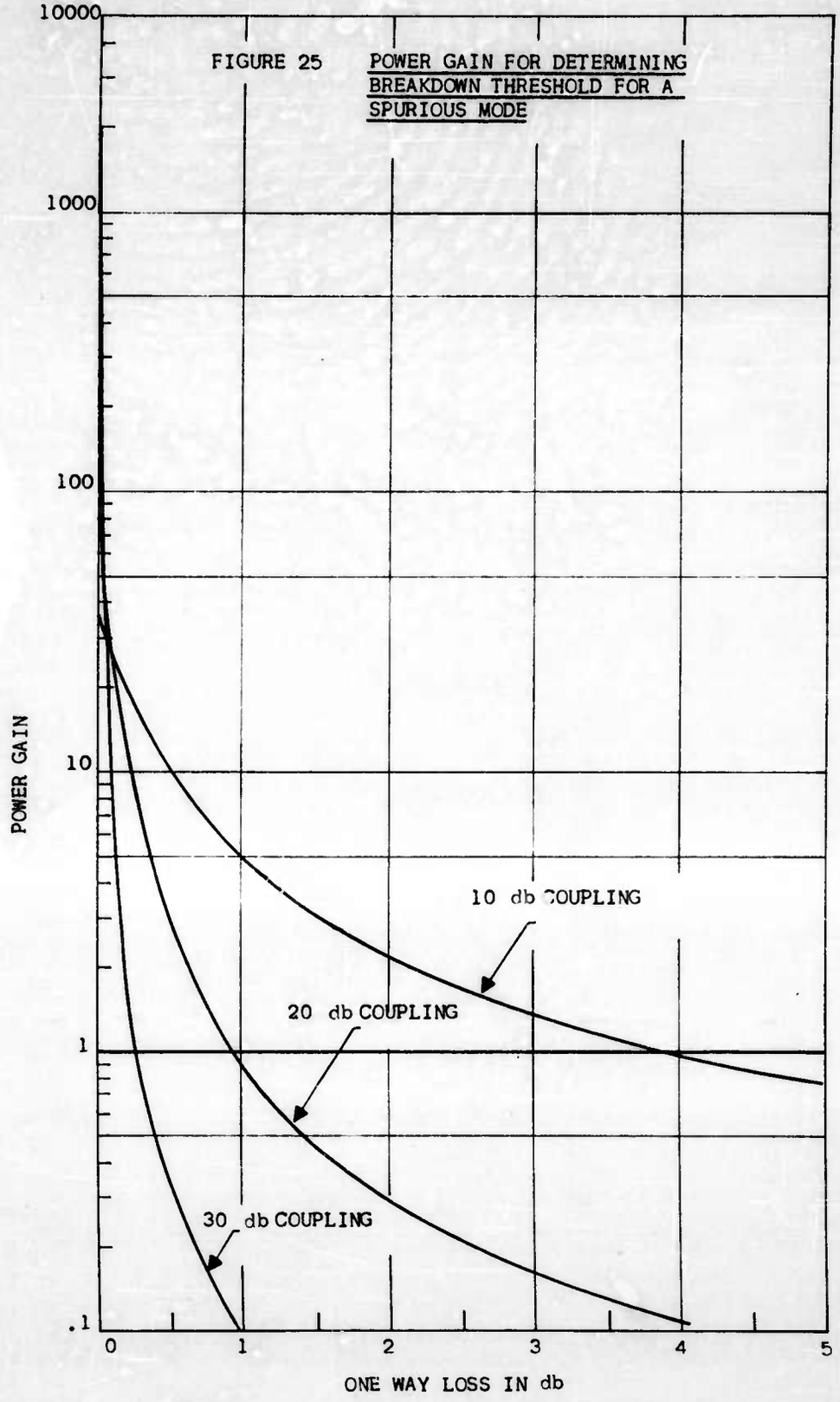

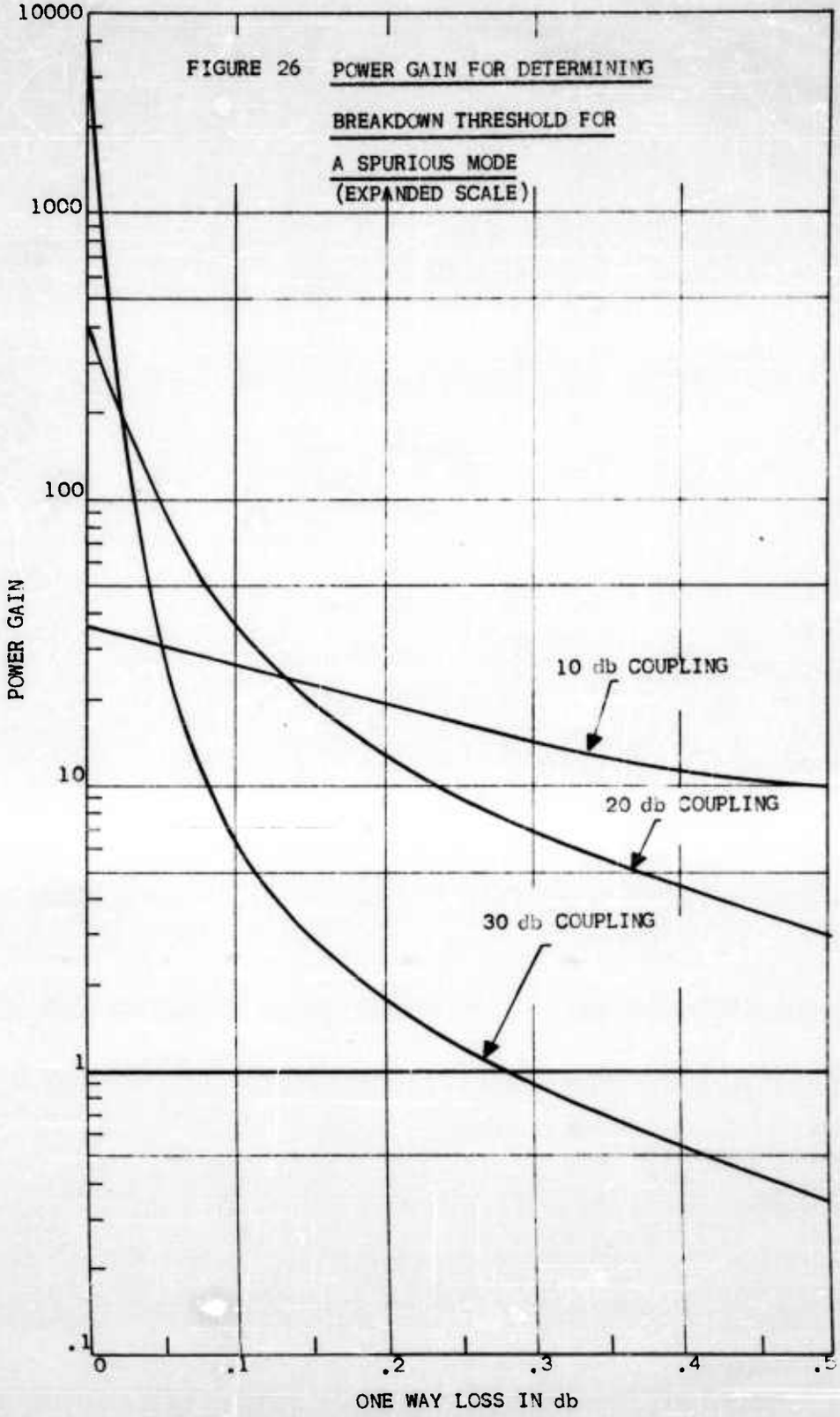

FIGURE 26 POWER GAIN FOR DETERMINING BREAKDOWN THRESHOLD FOR A SPURIOUS MODE (EXPANDED SCALE)

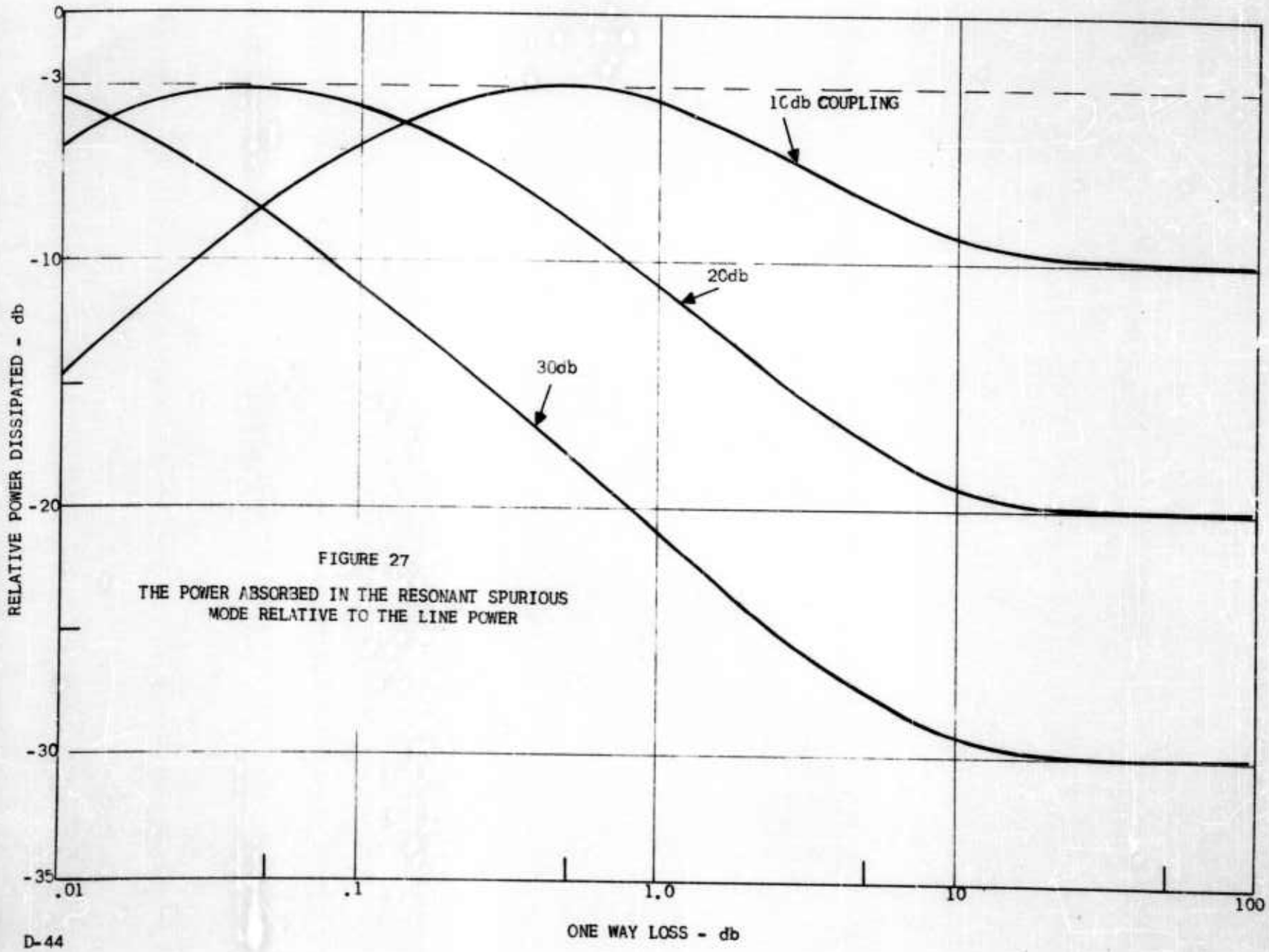

FIGURE 27

THE POWER ABSORBED IN THE RESONANT SPURIOUS MODE RELATIVE TO THE LINE POWER

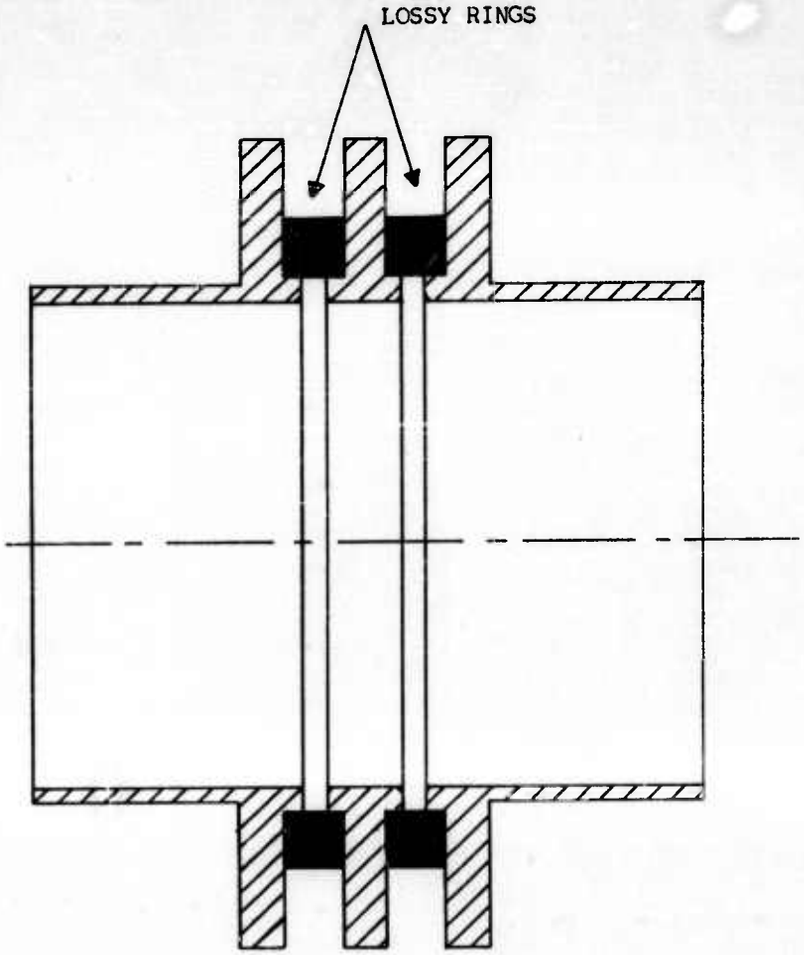

FIGURE 28

HIGH POWER MODE FILTER SECTION

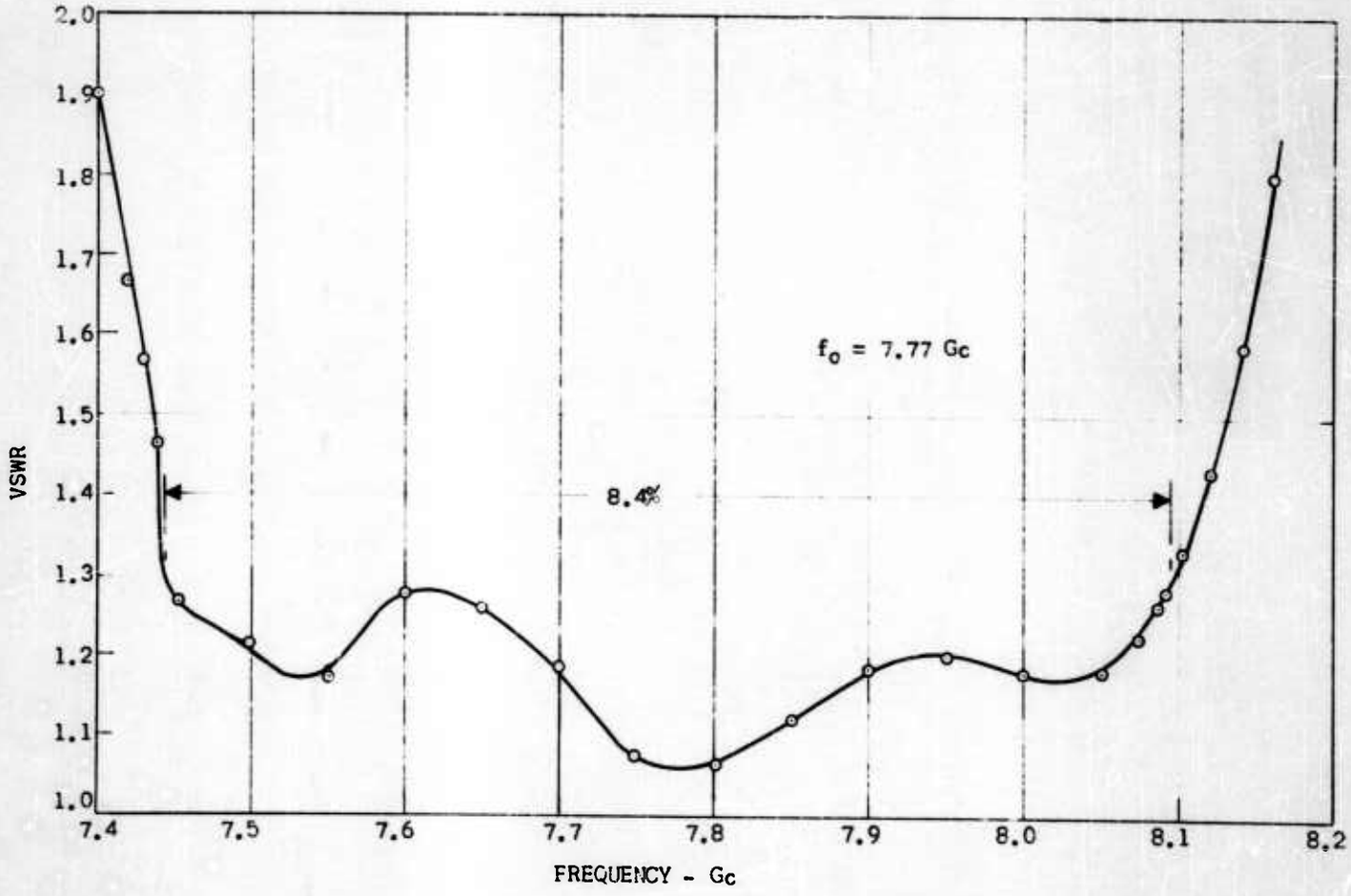

FIGURE 29

VSWR OF HIGH POWER MODE TRANSDUCER

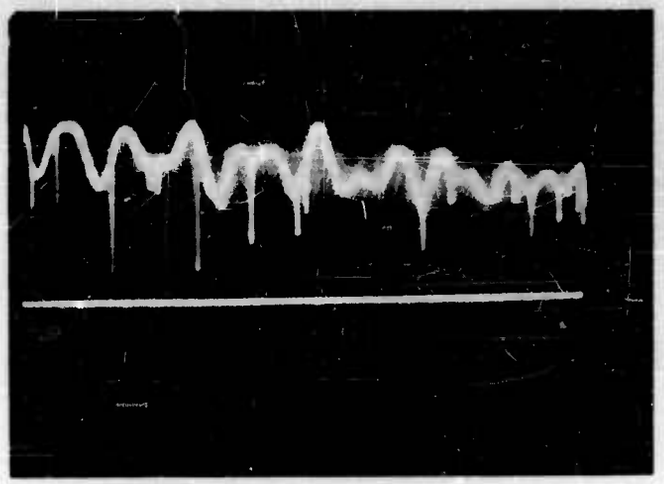

REFLECTED SIGNAL

Frequency

a.) Unfiltered example

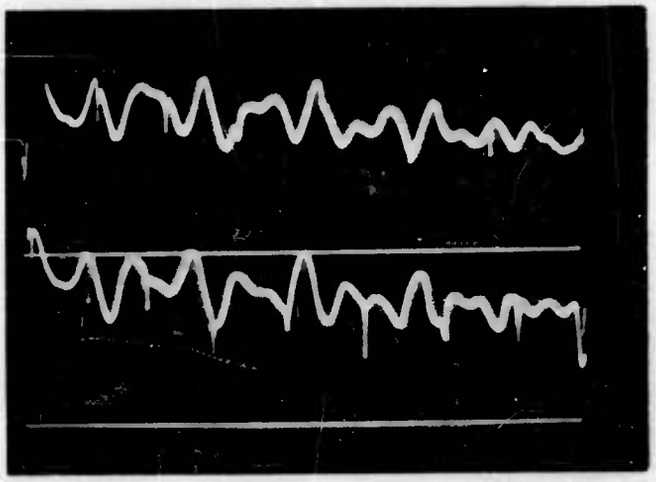

REFLECTED SIGNAL

Frequency

b.) Filtered examples
Upper trace - favorable position of short circuit
Lower trace - unfavorable position of short circuit

FIGURE 30
ATTENUATION OF SPURIOUS MODE RESONANCES ACROSS THE BAND BY A TWO SECTION MODE FILTER

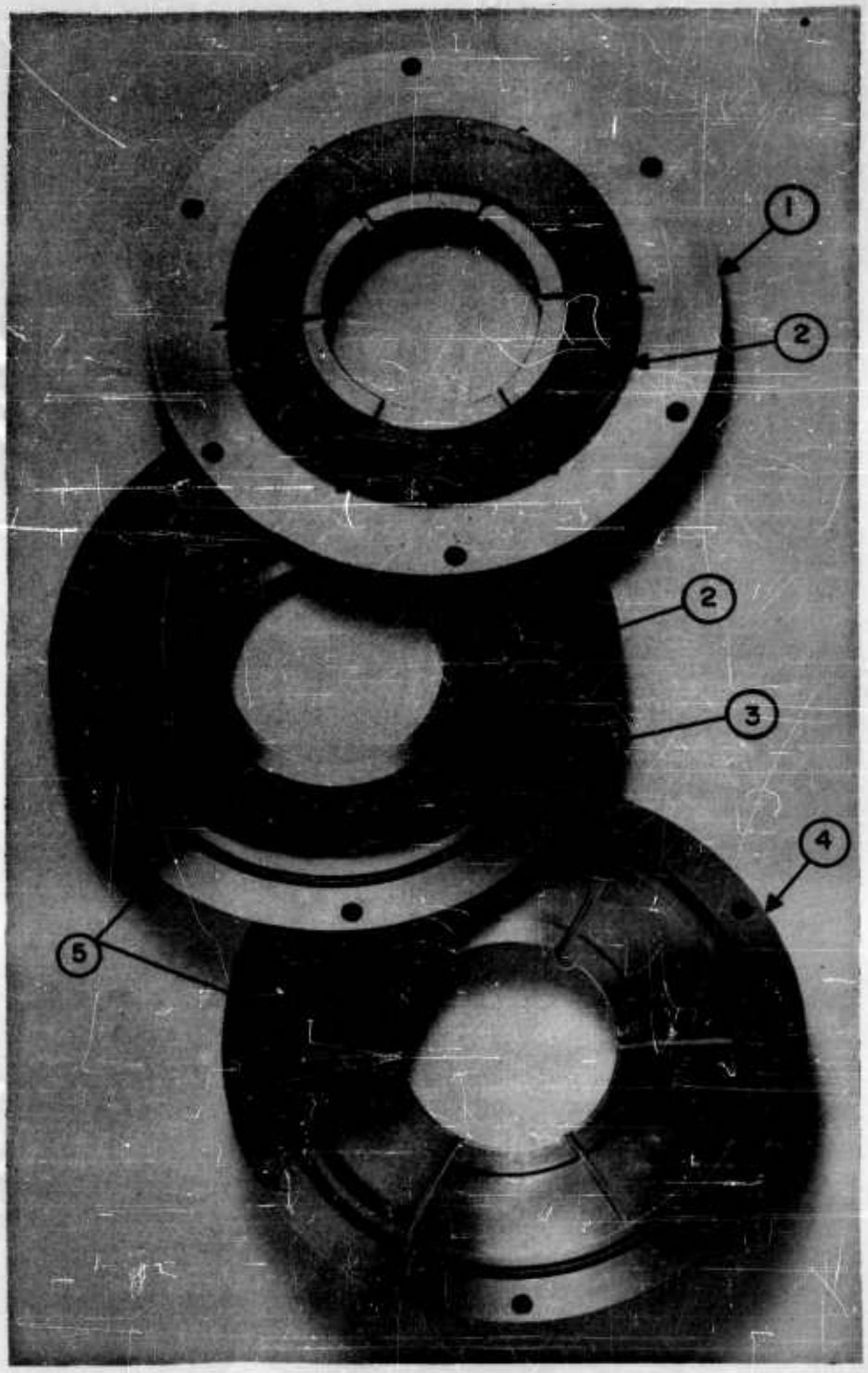

FIGURE 31 a
MODE FILTER PARTS-FINAL MODEL

ITEM	DESCRIPTION
1.	Center Flange
2.	Lossy Ring
3.	End Flange - Female
4.	End Flange - Male
5.	O - Rings

FIGURE 31b

MODE FILTER PARTS - FINAL MODEL

AD ——— Accession No. ———

MICROWAVE ASSOCIATES, INC.
Burlington, Massechusetts

ULTRA HIGH POWER TRANSMISSION LINE TECHNIQUES

Dr. Meyer Gilden, Richard Madore, Joseph Pergola

Finel Technicel Note

87 pp. - Illus. - Grapes, Air Force Contrect No. AF30(602)-2545

The ultre-high power transmission line techniques including both feilure mechanisme and component design are discussed. Feilures resulting from locelized regions of heated ges were studied and e more generel equetion for breekdown wes derived to show the effect of the size of the region. Similarly small obstscles produce regions of high field strength; but the presence of theee very small regions become evident only st high preesures or with high dielectric strength geses. Among the other subjects reviewed from earlier reports ie the experimentsl study of the fectors effecting arc movement in e wave-guide.

In view of the many edvantages of the low loss mode in circular weveguide for ultrs-high power levels, a mode transducer and e two section mode filter or suppreseor were designed and constructed. The short compact transducer has s bandwidth more than 8 percent end it can handle ebout 25 percent of the peak power of s standard rectenguler waveguide. Weter cooling is provided for high evsrege power operetion. Analysie of mode euppression ss relsted to fsilure of waveguide syetsme indicstee that an equivslent one way sttenuation of 5 db is a prsctical vslue of sttenuation for s mode suppressor where high sverags power levels are involved. Whsre only high pesk powers are involved lowsr levsle of attenuation ars eufficient.

UNCLASSIFIED

1. Ultre High Power Trans-mission Lina Techniques
2. Contract No. AF30(602) 2545

AD ——— Accession No. ———

MICROWAVE ASSOCIATES, INC.
Burlington, Massachusette

ULTRA HIGH POWER TRANSMISSION LINE TECHNIQUES

Dr. Meyer Gilden, Richard Madore, Josaph Pergola

Final Technicel Note

87 pp. - Illus. - Grsphs, Air Force Contrect No. AF30(602)-2545

Tha ultra-high power transmission line techniquee including both failure mechanisms and component dasign are discussed. Failures resulting from localized regions of heeted gae were studied and a more general equation for breakdown was derived to ehow tha effect of tba size of the region. Similarly small obstaclas produce regions of high field strength; but the presenca of these very small regions become evident only at high pressures or with high dielectric strength gssses. Among the other subjects reviewed from earlier reports is the experimental study of the fectors affecting arc movement in a wave-guids.

In view of the many edvantages of the low loss mode in circular waveguide for ultre-high power levels, a mode transducer and a two section mode filtar or suppreseor were designed and constructed. The short compact transducer has a bandwidth mora than 8 percent and it can handls ebout 25 percent of the peak power of a standard rectangular waveguide. Water cooling is provided for high averags power operstion. Analysis of mode suppression as related to failure of waveguide systems indicatee that an equivalent one way attenuation of 5 db ie a practical value of attenuation for a moda supprssssor whers high sverage power lavals ara involved. Whara only high peak powers ars involved lower levsls of attenuation ara sufficient.

UNCLASSIFIED

1. Ultre High Power Trans-miseion Line Techniques
2. Contract No. AF30(602) 2545

AD ——— Accession No. ———

MICROWAVE ASSOCIATES, INC.
Burlington, Maseachusetts

ULTRA HIGH POWER TRANSMISSION LINE TECHNIQUES

Dr. Meyer Gilden, Richard Madore, Joseph Pergols

Final Technicel Note

87 pp. - Illus. - Grephs, Air Force Contract No. AF30(602)-2545

The ultre-high power transmission line techniques including both feilure mechanisms and component design ere discussed. Fsilures resulting from localized regions of hested ges were studied and a more generel equetion for breakdown was derived to show the effect of the size of the region. Similarly small obstecles produce regions of high field strength; but the presence of these very small regions become evident only st high pressuree or with high dielectric strength geses. Among the other subjects reviewed from earlier reports ie the experimentsl study of the fectors effecting arc movement in s weve-guide.

In view of the many advantages of tbe low loss mode in circular weveguide for ultrs-high power levels, s mode transducer end a two section mode filter or suppressor were designed and constructed. The short compact transducer has e bandwidth more than 8 percent and it cen handls sbout 25 percent of the paek power of s standard rectenguler waveguids. Weter cooling is provided for high sverage power operstion. Analysis of mode suppresaion es related to fsilure of waveguide systsms indicetes that an equivelent one wey ettenuation of 5 db is a prsctical value of sttenuetion for s mode suppressor where high sverege power levels are involved. Where only high peek powers are involved lower levels of attenuation are sufficient.

UNCLASSIFIED

1. Ultra High Power Trans-mission Lins Techniques
2. Contract No. AF30(602) 2545

AD ——— Acasssion No. ———

MICROWAVE ASSOCIATES, INC.
Burlington, Massachueetts

ULTRA HIGH POWER TRANSMISSION LINE TECHNIQUES

Dr. Meyer Gilden, Richard Madore, Joseph Pergola

Final Technicel Note

87 pp. - Illus. - Grsphs, Air Force Contract No. AF30(602)-2545

The ultra-high power transmission lina techniquse including both failure mechanisms and component deeign are discussed. Failures raeulting from locslized regions of heeted gss wars etudied and a mors general equation for breakdown was derived to show the effect of the size of the region. Similarly small obstaclee produce regione of high field etrength; but the presence of these very small regions become evidant only et bigh pressuras or with high dialectric strength gasee. Among the other subjects reviewed from earlier reports is the sxperimental etudy of the factors effecting arc movement in a wave-guids.

In view of the many edventagss of the low loss moda in circular wavsguids for ultrs-high power lavsls, a mode transducer and a two section mode filter or suppressor were deeigned and constructed. Tha short compact transducer has a bandwidth more than 8 percent and it can handle ebout 25 percent of the peak power of a standard rectangular wavsguide. Water ccoling is provided for high average power operetion. Analysis of mode suppression ae related to failure of waveguide eystams indicatee that an equivalent one way attenuation of 5 db ie e practical vslue of attenuation for a moda euppreesor where high aversge power levels ara involved. Where only high peak powere ara involved lower levels of attanuation are sufficisnt.

UNCLASSIFIED

1. Ultra High Power Trans-miseion Line Techniques
2. Contract No. AF30(602) 2545

AD ——— Accession No. ———

MICROWAVE ASSOCIATES, INC.
Burlington, Massechusetts

ULTRA HIGH POWER TRANSMISSION LINE TECHNIQUES

Dr. Meyer Gilden, Richard Madore, Joseph Pergola

Final Tschnical Note

87 pp. - Illus. - Grephs, Air Force Contract No. AF30(602)-2545

The ultre-high cower transmieeion line techniquee including both feilure mechanisms and component design are discussed. Feilures resulting from localized regions of heeted gee were studied and a more generel equetion for breakdown wae derived to show tha effect of the size of the region. Similarly small obetacles produce regions of high field etrength; but the presence of theee very small regions become evident only at high pressures or with high dielectric strength geses. Among the other eubjecte reviewed from eerlier reports is the experimentel study of the fectors effecting arc movement in e wave-guide.

In view of the many advantegee of the low loss mode in circular waveguide for ultre-high power levels, e mode transducer and e two section mode filter or suppreeeor were designed and constructed. The short compact transducer has e bandwidth more than 8 percent end it can handle about 25 percent of the peek power of a standerd rectanguler waveguide. Water cooling is provided for high everege power operation. Analysis of mode suppression as related to failure of waveguide systems indicetes that an equivelent one way attenuation of 5 db is e practical value of ettenuation for a mode suppreeeor where high everege power levels are involved. Where only high peak powers are involved lower levels of ettenuation are sufficiant.

UNCLASSIFIED

1. Ultre High Power Trans-miseion Line Techniques
2. Contract No. AF30(602) 2545

AD ——— Accession No. ———

MICROWAVE ASSOCIATES, INC.
Burlington, Maseachusetts

ULTRA HIGH POWER TRANSMISSION LINE TECHNIQUES

Dr. Meyer Gilden, Richard Madore, Joseph Pergola

Final Technicel Note

87 pp. - Illus. - Graphs, Air Force Contract No. AF30(602)-2545

The ultra-high power transmission line techniques including both failure mechanisms and component design are discuseed. Failures resulting from localized regions of heated ges were studied and a more general equation for breakdown wae derived to ehow the affect of the size of the region. Similarly emall obetacles produce regions of high field strength; but the presence of these very emall regions become evident only at high pressures or with high dialectric strength gasee. Among the other subjects reviewed from earlier reporte is the experimental etudy of the factors effecting arc movement in a wave-guide.

In view of the mary advantagee of the low loss mode in circular waveguide for ultra-high power levele, a mode transducer and a two section mode filter or suppressor were deeigned and constructed. Tha short compact transducar has a bandwidth more than 8 percent and it can handle about 25 percent of the peak power of a standard rectangular waveguide. Water cooling is provided for high averaga power operation. Analysis of moda suppression as related to failure of waveguide systems indicatas that an equivalent one way attenuation of 5 db is a practical value of attemation for a mode suppressor where high average power levele ara involved. Where only high peak powers are involved lower levele of attemation are sufficient.

UNCLASSIFIED

1. Ultre High Power Trans-miseion Line Techniques
2. Contract No. AF30(602) 2545

AD ——— Accession No. ———

MICROWAVE ASSOCIATES, INC.
Burlington, Messechusetts

ULTRA HIGH POWER TRANSMISSION LINE TECHNIQUES

Dr. Meyer Gilden, Richard Madore, Joseph Pergola

Final Technical Note

87 pp. - Illus. - Grephs, Air Force Contract No. AF30(602)-2545

The ultre-high power transmission line techniques including both failure mechanisms and component design are discussed. Feilures resulting from localized regions of heated ges were studied and e more general equetion for breakdown was derived to ehow the effect of the size of the region. Similarly small obstecles produce regione of high field etrength; but the presence of these very small regions become evident only et high pressures or with high dielectric strength geses. Among the other subjects reviewed from earlier reports is the sxperimental study of the fectors effecting arc movement in e wave-guide.

In view of the many edvantages of the low loes mode in circuler weveguide for ultre-high power levels, e mode transducer and e two section mode filter or suppressor were designed and constructed. The short compact transducer has e bandwidth mora than 8 percent end it can handle about 25 percent of the peek power of e standard rectanguler waveguide. Water cooling is provided for high everage power operetion. Amalysis of mods suppreseion ee related to feilure of weveguide systems indicetes that an equivelent one wey attenuation of 5 db is e practical value of attenuation for e mode euppressor whare high average power levels are involved. Where only high peak powers are involved lower levels of attenuation are eufficient.

UNCLASSIFIED

1. Ultra High Power Trans-miesion Line Techniques
2. Contract No. AF30(602) 2545

AD ——— Accession No. ———

MICROWAVE ASSOCIATES, INC.
Burlington, Maseachusetts

ULTRA HIGH POWER TRANSMISSION LINE TECHNIQUES

Dr. Meyar Gilden, Richard Madore, Joeeph Pergola

Final Technical Note

87 pp. - Illua. - Graphs, Air Force Contract No. AF30(602)-2545

The ultre-high power transmieeion line techniquee including both failure mechanisms and component deeign are diecussed. Failures resulting from localized regions of heeted gas were studied and a more general equation for breakdown wae derived to show the effect of the size of the region. Similarly emall obetacles produca regions of high field strength; but tha presence of thaea very small regions become evident only et high preesuras or with high dielectric etrength gases. Among the other subjects reviewed from earlier reporte is the experimental study of the factors effecting arc movement in a wave-guide.

In view of the many advantagee of the low loss moda in circular waveguide for ultra-high power levele, a mode transducer and a two section mode filter or suppressor were deeigned and constructed. The ehort compact transducer hae a bandwidth more than 8 percent and it can handle about 25 percent of the peak power of a etandard rectangular waveguide. Water cooling is provided for high everage powar operetion. Analysie of mode suppreeeion es related to failure of waveguide eystems indicates thet an equivalent one way attenuation of 5 db is a practical value of attenuation for a moda euppreeeor where high average power levels are involved. Whera only high peak powere are involved lower levels of attenuation ara sufficient.

UNCLASSIFIED

1. Ultra High Power Trans-mission Line Techniques
2. Contract No. AF30(602) 2545

Final Report on Contract AF 30(602)2545

DISTRIBUTION LIST

	No. of Copies
Rome Air Development Center Griffiss Air Force Base Rome, New York Attn: RALTM Mr. Vannicola	3
Rome Air Development Center Griffiss Air Force Base Rome, New York Attn: RAAPT	1
Rome Air Development Center Griffiss Air Force Base Rome, New York Attn: RAALD	1
Rome Air Development Center Griffiss Air Force Base Rome, New York Attn: GEEIA (ROZMCAT)	1
Rome Air Development Center Griffiss Air Force Base Rome, New York Attn: RAIS, Attn: Mr. Malloy	1
U.S. Army Electronics R&D Labs Liaison Officer Rome Air Development Center Griffiss Air Force Base Rome, New York	1
AUL (3T) Maxwell Air Force Base Alabama	1
ASD (ASAPRD) Wright-Patterson Air Force Base Dayton, Ohio	1
Chief Naval Research Lab. Washington 25, D. C. Attn: Code 2027	1

	No. of Copies
Air Force Field Representative Naval Research Lab. Washington 25, D. C. Attn: Code 1010	1
Commanding Officer U. S. Army Electronics R&D Labs Fort Monmouth, New Jersey Attn: SELRA/SL-ADT	1
DDC (TISIA-2) Arlington Hall Station Arlington 12, Virginia	10
AFSC (SCSE) Andrews Air Force Base Washington 25, D. C.	1
Commanding General U.S. Army Electronic Proving Ground Ft. Huachuca, Arizona Attn: Technical Documents Library	1
AFPR General Electric Company Lockland Branch P.O.Box 91 Cincinnati 15, Ohio	1
Chief, Bureau of Ships Department of the Navy Washington 25, D. C. Attn: 312	1
Office of the Chief Signal Officer Department of the Army Washington 25, D. C. Attn: SIGRD	1
Dielectric Products Company Raymond, Maine Attn: Dr. Charles Brown	1

	No. of Copies
Armour Research Foundation of Illinois Institute of Technology Chicago 16, Illinois Attn: J. E. McManus	1
Kane Engineering Corporation Palo Alto, California Attn: Dr. Kane	1
Sperry Gyroscope Company Lake Success, New York Attn: Lenard Swern	1
Rome Air Development Center Griffiss Air Force Base Rome, New York Attn: RALTP/Mr. Quinn)	1
Rome Air Development Center Griffiss Air Force Base Rome, New York Attn: (RALSP/Mr. J. Cameron)	1
Rome Air Development Center Griffiss Air Force Base Rome, New York Attn: RALS/Mr. Dovydaitis	1
Rome Air Development Center Griffiss Air Force Base Rome, New York Attn: RALCD/Mr. Koegler	1
Advisory Group on Electronic Devices Working Group on Microwave Devices 346 Broadway New York, New York Attn: Mr. W. Kramer	1
Commanding Officer USASRDL Fort Monmouth, New Jersey Attn: SIGRA/SL-PEE/Mr. Lipetz	1

	No. of Copies
Bureau of Ships - 691B2C Electronics Division Room 3329 Main Navy Building Washington 25, D. C. Attn: Mr. Leo V. Gumina	1
Airborne Instruments Laboratory Deer Park, Long Island New York Attn: Mr. Avery	1
General Electric Company Heavy Military Electronics Department Syracuse, New York Attn: Dr. Joseph C. Almasi	1
ESK L. G. Hanscom Field Bedford, Massachusetts Attn: S. Herskovitz	1
Scientific Engineering Institute 140 Fourth Avenue Waltham, Massachusetts Attn: Mr. Daniel Schwarzkoph	1
Cornell Aeronautical Laboratory Buffalo, New York Attn: Mr. Beitz	1
General Engineering Lab. Schenectady, New York Attn: George E. Feiker	1
Sperry Gyroscope Company Mail Sta. D-40 Great Neck, New York Attn: Frank Liebert	1